Inorg. Chem. **2002**, *41*, 6474–6487

Novel Rectangular $[Fe_4(\mu_4\text{-}OHO)(\mu\text{-}OH)_2]^{7+}$ versus "Butterfly" $[Fe_4(\mu_3\text{-}O)_2]^{8+}$ Core Topology in the Fe^{III}/RCO_2^-/phen Reaction Systems (R = Me, Ph; phen = 1,10-Phenanthroline): Preparation and Properties of $[Fe_4(OHO)(OH)_2(O_2CMe)_4(phen)_4](ClO_4)_3$, $[Fe_4O_2(O_2CPh)_7(phen)_2](ClO_4)$, and $[Fe_4O_2(O_2CPh)_8(phen)_2]$

Athanassios K. Boudalis,[1a,†] Nikolia Lalioti,[1b] Georgios A. Spyroulias,[1c] Catherine P. Raptopoulou,[1d] Aris Terzis,[1d] Azzedine Bousseksou,[1e] Vassilis Tangoulis,[1b] Jean-Pierre Tuchagues,*[,1e] and Spyros P. Perlepes*[,1a]

Department of Chemistry, University of Patras, 26504 Patras, Greece, Department of Materials Science, University of Patras, 26504 Patras, Greece, Department of Pharmacy, University of Patras, 26504 Patras, Greece, Institute of Materials Science, NCSR "Demokritos", 15310 Aghia Paraskevi Attikis, Greece, and Laboratoire de Chimie de Coordination du CNRS, UPR 8241, 205 route de Narbonne, 31077 Toulouse Cedex 04, France

Received June 17, 2002

The preparations, X-ray structures, and detailed physical characterizations are presented for three new tetranuclear Fe^{III}/RCO_2^-/phen complexes, where phen = 1,10-phenanthroline: $[Fe_4(OHO)(OH)_2(O_2CMe)_4(phen)_4](ClO_4)_3\cdot 4.4MeCN\cdot H_2O$ (**1**·4.4MeCN·H_2O); $[Fe_4O_2(O_2CPh)_7(phen)_2](ClO_4)\cdot 2MeCN$ (**2**·2MeCN); $[Fe_4O_2(O_2CPh)_8(phen)_2]\cdot 2H_2O$ (**3**·$2H_2O$). Complex **1**·4.4MeCN·H_2O crystallizes in space group $P2_1/n$, with $a = 18.162(9)$ Å, $b = 39.016(19)$ Å, $c = 13.054(7)$ Å, $\beta = 104.29(2)°$, $Z = 4$, and $V = 8963.7$ Å^3. Complex **2**·2MeCN crystallizes in space group $P2_1/n$, with $a = 18.532(2)$ Å, $b = 35.908(3)$ Å, $c = 11.591(1)$ Å, $\beta = 96.42(1)°$, $Z = 4$, and $V = 7665(1)$ Å^3. Complex **3**·$2H_2O$ crystallizes in space group $I2/a$, with $a = 18.79(1)$ Å, $b = 22.80(1)$ Å, $c = 20.74(1)$ Å, $\beta = 113.21(2)°$, $Z = 4$, and $V = 8166(1)$ Å^3. The cation of **1** contains the novel $[Fe_4(\mu_4\text{-}OHO)(\mu\text{-}OH)_2]^{7+}$ core. The core structure of **2** and **3** consists of a tetranuclear bis(μ_3-O) cluster disposed in a "butterfly" arrangement. Magnetic susceptibility data were collected on **1**–**3** in the 2–300 K range. For the rectangular complex **1**, fitting the data to the appropriate theoretical χ_M vs T expression gave $J_1 = -75.4$ cm^{-1}, $J_2 = -21.4$ cm^{-1}, and $g = 2.0(1)$, where J_1 and J_2 refer to the $Fe^{III}O(O_2CMe)_2Fe^{III}$ and $Fe^{III}(OH)Fe^{III}$ pairwise exchange interactions, respectively. The $S = 0$ ground state of **1** was confirmed by 2 K magnetization data. The data for **2** and **3** reveal a diamagnetic ground state with antiferromagnetic exchange interactions among the four high-spin Fe^{III} ions. The exchange coupling constant J_{bb} ("body–body" interaction) is indeterminate due to prevailing spin frustration, but the "wing–body" antiferromagnetic interaction (J_{wb}) was evaluated to be –77.6 and –65.7 cm^{-1} for **2** and **3**, respectively, using the appropriate spin Hamiltonian approach. Mössbauer spectra of **1**–**3** are consistent with high-spin Fe^{III} ions. The data indicated asymmetry of the Fe_4 core of **1** at 80 K, which is not detected at room temperature due to thermal motion of the core. The spectra of **2** and **3** analyze as two quadrupole-split doublets which were assigned to the body and wing-tip pairs of metal ions. ^{1}H NMR spectra are reported for **1**–**3** with assignment of the main resonances.

Introduction

Dinuclear and polynuclear hydroxo-, alkoxo- and oxo-bridged iron(III) complexes are of current interest from a variety of viewpoints, including molecular magnetic materials and bioinorganic chemistry. In the former area it has been found that some of these clusters possess large total spin values (S) in their ground state,[2] a property resulting from the existence of at least some intramolecular exchange interactions that are ferromagnetic in nature and/or the presence of spin frustration effects. The large S value

* To whom correspondence should be addressed. E-mail: perlepes@patreas.upatras.gr (S.P.P.); tuchague@lcc-toulouse.fr (J.-P.T.).
† Temporary address: Laboratoire de Chimie de Coordination du CNRS, UPR 8241, 205 route de Narbonne, 31077 Toulouse Cedex 04, France.

10.1021/ic025795k CCC: $22.00 © 2002 American Chemical Society
Published on Web 11/02/2002

provides the possibility of obtaining new examples of iron-based single-molecule magnets (SMMs), i.e., molecular species which show a slow relaxation rate of the magnetization.[3] For example, the smallest iron(III) SMM is $[Fe_4(OMe)_6(dpm)_6]$,[4] where dpm^- is the anion of dipivaloylmethane, exhibiting a $S = 5$ ground state. In the bioinorganic area, hydroxo- and oxo-bridged dinuclear complexes represent synthetic models of the active sites of various non-heme iron proteins[5] such as hemerythrin (Hr), ribonucleotide reductase R2 protein (RNR-R2), the hydroxylase component of methane monooxygenase (MMOH), and fatty acyl desaturases, which contain diiron cores bridged by oxo or hydroxo ligands. From another bioinorganic chemistry point of view, polynuclear Fe^{III}/O^{2-}, OH^- complexes represent model systems for the buildup of the iron−oxo core of ferritin[6] or for biomineralization processes that form a variety of iron−oxo minerals such as ferrihydrite, goethite, etc.[7]

Important to the future of the above areas is the development of synthetic procedures that can yield new Fe^{III} hydroxo/alkoxo/oxo dinuclear and polynuclear complexes. The ability of the ligand systems $RCO_2^-/L-L$ (L−L = neutral bidentate N-donor) to assemble novel Fe^{III}_x cluster types ($x = 2-6$) exhibiting aesthetically pleasing structures and interesting magnetic phenomena (e.g., spin frustration) has been investigated. Restricting further discussion to L−L = 2,2′-bipyridine (bpy), 1,10-phenanthroline (phen), or their derivatives, the up to now structurally characterized members of this family are $[Fe_2O(O_2CMe)_2Cl_2(bpy)_2]$,[8a] $[Fe_2O(O_2CCH_2Cl)_2(H_2O)(bpy)_2](NO_3)_2$,[8b] $[Fe_4O_2(O_2CMe)_7(bpy)_2]X$ (X = ClO_4,[9a] Cl[9b]), $[Fe_4O_2(O_2CEt)_7(bpy)_2]X$ (X = ClO_4,[9c] PF_6[9d]), $[Fe_4O_2Cl_2(O_2CMe)_6(bpy)_2]$,[9e] $[Fe_6O_3(OEt)_2(O_2CMe)_9(bpy)_2](ClO_4)$,[10] $[Fe_2O(O_2CCF_3)_2(Me_2bpy)_4](ClO_4)_2$[11] ($Me_2bpy$ = 4,4′-dimethyl-2,2′-bipyridine), $[Fe_2O(O_2CPh)_2(phen)_4]Cl_2$,[12] $[Fe_3O_2(O_2CMe)_2(phen)_6](ClO_4)_3$,[13] and $Na[Fe_6O_4(OH)_2(ami)_4(phen)_8](NO_3)_9$[14] (ami = the zwitterionic form of β-alanine).

Two observations concerning the above family have been the stimuli of our efforts. First, we noticed that the Fe^{III}: L−L (L−L = bpy, phen) ratio in the tri-, tetra- and hexanuclear clusters is 3:1, 2:1, 1:2, or 3:4; no 1:1 clusters have been reported. And second, contrary to the numerous tetranuclear Fe^{III}/RCO_2^-/bpy complexes, no such iron(III) carboxylate clusters with phen are known. The former all have the $[Fe_4(\mu_3\text{-}O)_2]^{8+}$ core. Tetranuclear, oxide-bridged carboxylate clusters of Fe^{III} containing this core have been under study for several years yielding a wealth of structural, spectroscopic, and physical data. Almost all known examples have either the bent ("butterfly")[9d-e,15]or planar[16] dispositions of four Fe^{III} atoms, types **I** and **II**, respectively, with the pyramidal μ_3-O^{2-} ions either on the same side (**I**) or on opposite sides (**II**) of the fused Fe_3 planes. $[Fe_4O_2Cl_2(O_2CMe)_6Cl_2(bpy)_2]$ displays an unusual structural asymmetry in its core that can be described as a hybrid of the bent and planar dispositions of the four metal ions (**III**).[9e]

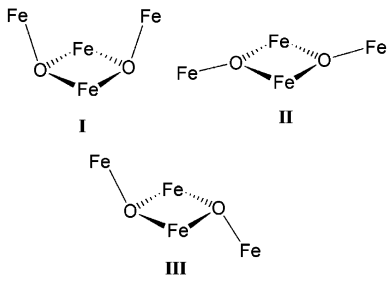

(1) (a) Chemistry Department, University of Patras. (b)Department of Materials Science, University of Patras. (c) Department of Pharmacy, University of Patras. (d) NCSR "Demokritos". (e) Laboratoire de Chimie de Coordination.

(2) (a) Powell, A. K.; Heath, S. L.; Gatteschi, D.; Pardi, L.; Sessoli, R.; Spina, G.; Del Giallo, F.; Pieralli, F. *J. Am. Chem. Soc.* **1995**, *117*, 2491. (b) Goodwin, J. C.; Sessoli, R.; Gatteschi, D.; Wernsdorfer, W.; Powell A. K.; Heath S. L. *J. Chem. Soc., Dalton Trans.* **2000**, 1835. (c) McCusker, J. K.; Christmas, C. A.; Hogen, P. M.; Chadha, R. K.; Harvey, D. F.; Hendrickson, D. N. *J. Am. Chem. Soc.* **1991**, *113*, 6114. (d) Christmas, C. A.; Tsai, H.-L.; Pardi, L.; Kesselman, J. L.; Gantzel, P. K.; Chadha, R. K.; Gatteschi, D.; Harvey, D. F.; Hendrickson, D. N. *J. Am. Chem. Soc.* **1993**, *115*, 12483. (e) Delfs, C.; Gatteschi, D.; Pardi, L.; Sessoli, R.; Wieghardt, K.; Hanke, D. *Inorg. Chem.* **1993**, *132*, 3099.

(3) (a) Gatteschi, D.; Sessoli, R.; Cornia, A. *Chem. Commun.* **2000**, 725. (b) Christou, G.; Gatteschi, D.; Hendrickson, D. N.; Sessoli, R. *MRS Bull.* **2000**, *25*, 1.

(4) Barra, A. L.; Caneschi, A.; Cornia, A.; Fabrizi de Biani, F.; Gatteschi, D.; Sangregorio, C.; Sessoli, R.; Sorace, L. *J. Am. Chem. Soc.* **1999**, *121*, 5302.

(5) (a) Kurtz, D. M., Jr. *J. Biol. Inorg. Chem.* **1997**, *2*, 159. (b) Nordlund, P.; Eklund, H. *Curr. Opin. Struct. Biol.* **1995**, *5*, 758. (c) Que, L., Jr. *J. Chem. Soc., Dalton Trans.* **1997**, 3933. (d) Logan, D. T.; Su, X.-D.; Aberg, A.; Regnsträn, K.; Hajdu, J.; Eklund, H.; Nordlund, P. *Structure* **1996**, *4*, 1053. (e) Rosenzweig, A. C.; Nordlund, P.; Takahara, P. M.; Frederick, C. A. *Chem. Biol.* **1995**, *2*, 409. (f) Lindqvist, Y.; Huang, W.; Schneider, G.; Shanklin, J. *EMBO J.* **1996**, *15*, 4081. (g) Que, L., Jr. *Chem. Rev.* **1996**, *96*, 2607.

(6) (a) Clegg, G. A.; Fitton, J. E.; Harrison, P. M.; Treffry, A. *Prog. Biophys. Mol. Biol.* **1980**, *36*, 53. (b) Theil, E. C. *Annu. Rev. Biochem.* **1987**, *56*, 289. (c) Harrison, P. M.; Arosio, P. *Biochim. Biophys. Acta* **1996**, *1275*, 161.

(7) *Biomineralization: Chemical and Biochemical Perspectives*; Mann, S., Webb, J., Williams, R. J. P., Eds.; VCH Publishers: New York, 1988.

(8) (a) Vincent, J. B.; Huffman, J. C.; Christou, G.; Li, Q.; Nanny, M. A.; Hendrickson, D. N.; Fong, R. H.; Fish, R. H. *J. Am. Chem. Soc.* **1988**, *110*, 6898. (b) Taft, K. L.; Maschelein, A.; Liu, S.; Lippard, S. J.; Garfinkel-Shweky, D.; Bino, A. *Inorg. Chim. Acta* **1992**, *198*−*200*, 627.

(9) (a) McCusker, J. K.; Vincent, J. B.; Schmitt, E. A.; Mino, M. L.; Shin, K.; Coggin, D. K.; Hagen, P. M.; Huffman, J. C.; Christou, G.; Hendrickson, D. N. *J. Am. Chem. Soc.* **1991**, *113*, 3012. (b) Pan, W.-Y.; Yu, X.-F. *Chin. J. Chem.* **1994**, *12*, 534. (c) Yu, X.-F.; Jiang, Y.-Q. *Huaxue Xuebao* **1993**, *51*, 579. (d) Yan, B.; Chen, Z.-D. *Inorg. Chem. Commun.* **2001**, *4*, 138. (e) Wemple, M. W.; Coggin, D. K.; Vincent, J. B.; McCusker, J. K.; Streib, W. E.; Huffman, J. C.; Hendrickson, D. N.; Christou, G. *J. Chem. Soc., Dalton Trans.* **1998**, 719.

(10) Seddon, E. J.; Huffman, J. C.; Christou, G. *J. Chem. Soc., Dalton Trans.* **2000**, 4446.

(11) Ménage, S.; Vincent, J.-M.; Lambeaux, C.; Chottard, G.; Grand A.; Fontecave, M. *Inorg. Chem.* **1993**, *32*, 4766.

(12) Li, J.; Zou, J.; Wu, M.; Xu, Z.; You, X.; Mak, T. C. W. *Polyhedron* **1995**, *14*, 3519.

(13) Vincent, J.-M.; Ménage, S.; Latour J.-M.; Bousseksou, A.; Tuchagues, J.-P.; Decian, A.; Fontecave, M. *Angew. Chem., Int. Ed. Engl.* **1995**, *34*, 205.

(14) Tokii, T.; Ide, K.; Nakashima, M.; Koikawa, X. *Chem. Lett.* **1994**, 441.

(15) (a) Armstrong, W. H.; Roth, M. E.; Lippard, S. J. *J. Am. Chem. Soc.* **1987**, *109*, 6318. (b) Chaudhuri, P.; Winter, M.; Fleischhauer, P.; Haase, W.; Florke, U.; Haupt, H.-J. *Inorg. Chim. Acta* **1993**, *212*, 241. (c) Wu, L.; Pressprich, P.; Coppens, P.; DeMarco, M. J. *Acta Crystallogr., Sect. C* **1993**, *49*, 1255. (d) Reynolds, R. A., III; Dunham, W. R.; Coucouvanis, D. C. *Inorg. Chem.* **1998**, *37*, 1232.

(16) (a) Ponomarev, V. I.; Atovmyan, L. O.; Bobkova, S. A.; Turte, K. I. *Dokl. Akad. Nauk. SSSR* **1984**, *274*, 368. (b) Gorun, S. M.; Lippard, S. J.; *Inorg. Chem.* **1988**, *27*, 149. (c) Celenligil-Cetin, R.; Staples, R. J.; Stavropoulos, P. *Inorg. Chem.* **2000**, *39*, 5838.

Suspecting that 1:1 Fe^{III}:phen clusters and tetranuclear species possessing the $[Fe_4(\mu_3\text{-}O)_2]^{8+}$ core could exist, we concentrated our efforts on the Fe^{III}/O^{2-}, OH^-/RCO_2^-/phen chemistry. In this paper, we describe the preparation, X-ray crystal structures, magnetic properties, and spectroscopic (IR, ^{57}Fe-Mössbauer, ^{1}H NMR) characterization of complexes $[Fe_4(OHO)(OH)_2(O_2CMe)_4(phen)_4](ClO_4)_3$ (**1**), $[Fe_4O_2(O_2CPh)_7(phen)_2](ClO_4)$ (**2**), and $[Fe_4O_2(O_2CPh)_8(phen)_2]$ (**3**). Complex **1** is the desired 1:1 Fe^{III}:phen carboxylate cluster containing the novel $[Fe_4(\mu_4\text{-}OHO)(\mu\text{-}OH)_2]^{7+}$ core, while complexes **2** and **3** are the first members of the Fe^{III}/RCO_2^-/phen subfamily of clusters with the $[Fe_4(\mu_3\text{-}O)_2]^{8+}$ core. In addition, we report reactivity studies with the goal to assess the basic chemistry underlying the isolated clusters, i.e., pathways between the different types of complexes. The structure and preliminary magnetic properties of **1** have been briefly communicated.[17] This work is the continuation of a broad program[18] concerned with developing synthetic routes to, and studying the magnetic properties of, polynuclear complexes of 3d-metals at intermediate oxidation states. Polynuclear 3d-metal chemistry is today an area of modern science whose interfaces with many disciplines have provided invaluable opportunities for crossing boundaries both inside and between the fields of chemistry, biology, and physics.

Experimental Section

Syntheses. All manipulations were performed under aerobic conditions using reagents and solvents as received (Aldrich Co.) Basic iron(III) benzoate was prepared as described elsewhere.[19]

Caution! Although no such behavior was observed during the present work, perchlorate salts are potentially explosive and should be handled with care.

$[Fe_4(OHO)(OH)_2(O_2CMe)_4(phen)_4](ClO_4)_3\cdot 4.4MeCN\cdot H_2O$ (1·4.4MeCN·H_2O). To a stirred deep red solution of $Fe(ClO_4)_3\cdot 6H_2O$ (6.93 g, 15.0 mmol) and $NaO_2CMe\cdot 3H_2O$ (3.57 g, 26.2 mmol) in MeCN (35 mL) was added a solution of phen·H_2O (2.97 g, 15.0 mmol) in the same solvent (19 mL). A noticeable color change to dark green occurred, and the solution soon began to deposit a dark green microcrystalline precipitate. The solid was collected by filtration, repeatedly washed with cold MeCN, and dried in vacuo. The yield was 4.12 g (~70%). X-ray-quality, green prismatic crystals of **1**·4.4MeCN·H_2O were grown from a similar reaction mixture, within 4−5 days, with the reactant concentrations scaled down to ca. 1/10. The dried sample analyzed as **1**·H_2O. Anal. Calcd for $C_{56}H_{49}Cl_3Fe_4N_8O_{25}$: C, 43.01; H, 3.16; N, 7.17. Found: C, 42.47; H, 3.19; N, 7.09. IR data (KBr pellet, cm^{-1}): 3414 (m, br), 3068 (w), 1570 (s), 1428 (s), 1342 (w), 1146 (w), 1107 (s), 1090 (s), 870 (w), 848 (m), 724 (s), 658 (w), 624 (m), 544 (w). The deuterated complex was prepared exactly as described for the normal complex using $Fe(ClO_4)_3\cdot 6D_2O$ (0.15 mmol) and $NaO_2CMe\cdot 3D_2O$ (0.26 mmol) and phen·D_2O (0.15 mmol) in MeCN (~1 mL); the sample was dried in vacuo at 40 °C.

$[Fe_4O_2(O_2CPh)_7(phen)_2](ClO_4)\cdot 2MeCN$ (2·2MeCN). Method A. To a stirred deep red solution of $Fe(ClO_4)_3\cdot 6H_2O$ (4.66 g, 10.1 mmol) and NaO_2CPh (2.54 g, 17.7 mmol) in MeCN (26 mL) was added a solution of phen·H_2O (2.00 g, 10.1 mmol) in the same solvent (6 mL). A color change to dark green occurred, and the solution soon began to deposit a dark green microcrystalline solid. The precipitate was collected by filtration, copiously washed with cold MeCN, and dried in air. The yield was 0.99 g (~25%). X-ray-quality, green-purple prismatic crystals of **2**·2MeCN were grown from a similar reaction mixture, within 2 weeks, with the reactant concentrations scaled down to ca. 1/2. The dried sample analyzed as **2**·MeCN. Anal. Calcd for $C_{75}H_{54}ClFe_4N_5O_{20}$: C, 56.16; H, 3.39; N, 4.37. Found: C, 56.09; H, 3.24; N, 4.13. IR data (KBr pellet, cm^{-1}): 3062 (w), 1710 (w), 1598 (s), 1554 (s), 1530 (m), 1520 (m), 1492 (w), 1446 (w), 1398 (s), 1176 (w), 1146 (w), 1106 (m), 1070 (w), 1024 (w), 870 (w), 848 (m), 724 (s), 674 (m), 648 (w), 624 (w), 602 (w), 520 (w), 472 (m).

Method B. To a stirred solution of **1**·H_2O (0.78 g, 0.5 mmol) in MeCN (10 mL) was added solid $PhCO_2H$ (0.43 g, 3.5 mmol). The solid soon dissolved, but no noticeable color change occurred. A strong smell of acetic acid was evident. A small quantity of dark green crystals of **2**·2MeCN formed after 24 h. These were collected by filtration, copiously washed with cold MeCN, and dried in air. Low yields of 5−8% were obtained.

Method C. To a stirred deep green solution of **1**·H_2O (0.31 g, 0.2 mmol) in MeCN (5 mL) were added solid PhO_2H (0.17 g, 1.4 mmol) and a solution of $NaClO_4\cdot H_2O$ (0.25 g, 1.8 mmol) in MeCN (5 mL). A deep green homogeneous solution was obtained from which green crystals of **2**·2MeCN began to precipitate after 12 h. When precipitation was judged to be complete, the product was collected by filtration, washed with cold MeCN, and dried in air. Yields were typically in the 40−45% range.

The identity of the products from methods B and C was confirmed by microanalyses (both dried samples analyzed as **2**·MeCN) and by IR spectroscopic comparison with samples from method A.

$[Fe_4O_2(O_2CPh)_8(phen)_2]\cdot 2H_2O$ (3·2H_2O). Basic iron(III) benzoate (0.76 g, 0.8 mmol), "$Fe_3(OH)O(O_2CPh)_6(H_2O)_2$", was dissolved in MeCN (10 mL) to yield a deep red solution, followed by the addition of solid phen·H_2O (0.24 g, 1.2 mmol). The latter dissolved immediately, and the solution turned brown-green. The reaction solution was stirred for 10 min and then filtered and left capped and undisturbed for 24 h. The resulting X-ray-quality, red prismatic crystals of **3**·2H_2O were collected on a frit, copiously washed with cold MeCN, and dried in vacuo. The yield was 40%. The dried compound analyzed as H_2O-free (**3**). Anal. Calcd for $C_{80}H_{56}Fe_4N_4O_{18}$: C, 60.63; H, 3.56; N 3.54. Found: C, 60.37; H, 3.69; N, 3.40. IR data (KBr pellet, cm^{-1}): 3060 (m), 3026 (w), 1637 (s), 1598 (s), 1558(s), 1518 (s), 1492 (m), 1446 (m), 1402 (s, br), 1176 (m), 1144 (m), 1106 (m), 1068 (m), 1026 (m), 870 (m), 846 (m), 720 (s), 688 (s), 674 (s), 656 (s), 596 (w), 574 (w), 518 (w), 468 (s).

(17) Boudalis, A. K.; Lalioti, N.; Spyroulias, G. A.; Raptopoulou, C. P.; Terzis, A.; Tangoulis, V.; Perlepes, S. P. *J. Chem. Soc., Dalton Trans.* **2001**, 955.

(18) (a) Papaefstathiou, G. S.; Escuer, A.; Vicente, R.; Font-Bardia, M.; Solans, X. *Chem. Commun.* **2001**, 2414. (b) Lalioti N.; Raptopoulou, C, P.; Terzis, A.; Aliev, A. E.; Gerothanassis, I. P.; Manessi-Zoupa, E.; Perlepes, S. P. *Angew. Chem., Int. Ed.* **2001**, *40*, 3211. (c) Papaefstathiou, G. S.; Escuer, A.; Raptopoulou, C. P.; Terzis, A.; Perlepes, S. P.; Vicente, R. *Eur. J. Inorg. Chem.* **2001**, 1567. (d) Papaefstathiou, G. S.; Perlepes, S. P.; Escuer, A.; Vicente, R.; Font-Bardia, M.; Solans, X. *Angew. Chem., Int. Ed.* **2001**, *40*, 884. (e) Papaefstathiou, G. S.; Raptopoulou, C. P.; Tsohos, A.; Terzis, A.; Bakalbassis, E. G.; Perlepes, S. P. *Inorg. Chem.* **2000**, *39*, 4658. (f) Tsohos, A.; Dionyssopoulou, S.; Raptopoulou, C. P.; Terzis, A.; Bakalbassis, E. G.; Perlepes, S. P. *Angew. Chem., Int. Ed.* **1999**, *38*, 983. (g) Tangoulis, V.; Raptopoulou, C. P.; Terzis, A.; Bakalbassis, E. G.; Diamantopoulou, E.; Perlepes, S. P. *Inorg. Chem.* **1998**, *37*, 3142. (h) Tangoulis, V.; Raptopoulou, C. P.; Paschalidou, S.; Bakalbassis, E. G.; Perlepes, S. P.; Terzis, A. *Angew. Chem., Int. Ed. Engl.* **1997**, *36*, 1083. (i) Tangoulis, V.; Raptopoulou, C. P.; Paschalidou, S.; Tsohos, A. E.; Bakalbassis, E. G.; Terzis, A.; Perlepes, S. P. *Inorg. Chem.* **1997**, *36*, 5270. (j) Tangoulis, V.; Raptopoulou, C. P.; Terzis, A.; Paschalidou, S.; Perlepes, S. P.; Bakalbassis, E. G. *Inorg. Chem.* **1997**, *36*, 3996.

(19) Earnshaw, A.; Figgis, B. N.; Lewis, J. *J. Chem. Soc. A* **1966**, 1656.

Table 1. Crystallographic Data for **1**−**3**

	1·4.4MeCN·H_2O	**2**·2MeCN	**3**·2H_2O
chem formula	$C_{64.8}H_{62.2}Cl_3Fe_4N_{12.4}O_{25}$	$C_{77}H_{57}ClFe_4N_6O_{20}$	$C_{80}H_{60}Fe_4N_4O_{20}$
fw	1744.22	1645.14	1620.72
space group	$P2_1/n$	$P2_1/n$	$I2/a$
a, Å	18.162(9)	18.532(2)	18.79(1)
b, Å	39.016(19)	35.908(3)	22.80(1)
c, Å	13.054(7)	11.591(1)	20.74(1)
β, deg	104.29(2)	96.42(1)	113.21(2)
V, Å^3	8963.7	7665(1)	8166(1)
Z	4	4	4
T, °C	25	25	25
λ, Å	0.710 73	1.541 80	0.710 73
D_{calcd}, g cm^{-3}	1.293	1.426	1.318
μ, mm^{-1}	0.796	6.905	0.766
R1[a]	0.0993	0.0737	0.0744
wR2[a]	0.2676	0.1897	0.1804

[a] $w = 1/[\sigma^2(F_o^2) + (aP)^2 + bP]$ and $P = (\max(F_o^2, 0) + 2F_c^2)/3$; $a = 0.1409$ and $b = 73.3684$ for **1**·4.4MeCN·H_2O, $a = 0.1157$ and $b = 32.2473$ for **2**·2MeCN, and $a = 0.0820$ and $b = 25.7531$ for **3**·2H_2O. R1 $= \Sigma(|F_o| - |F_c|)/\Sigma(|F_o|)$ and wR2 $= \{\Sigma[w(F_o^2 - F_c^2)^2]/\Sigma[w(F_o^2)^2]\}^{1/2}$ for 6721 (**1**·4.4MeCN·H_2O), 5328 (**2**·2MeCN), and 4438 (**3**·2H_2O) reflections with $I > 2\sigma(I)$.

Physical Measurements. Microanalyses were performed by the Microanalytical Laboratory of the Laboratoire de Chimie de Coordination at Toulouse. Infrared spectra (4000−400 cm^{-1}) were recorded as KBr disks on a Perkin-Elmer 16PC spectrometer. Room-temperature ^{1}H NMR spectroscopy was performed on a 400.13 MHz Avance DPX spectrometer (Bruker) using a spectral width of 120 ppm. Chemical shifts are quoted on the δ scale with respect to external TMS or the proton solvent signal. Mössbauer measurements were recorded on a constant-acceleration conventional spectrometer with a 50 mCi source of ^{57}Co (Rh matrix). The absorber was a powdered sample enclosed in a 20 mm diameter cylindrical, plastic sample-holder, the size of which had been determined to optimize the absorption. Variable-temperature spectra were obtained in the 80−300 K range, by using a MD 306 Oxford cryostat, the thermal scanning being monitored by an Oxford ITC4 servocontrol device (±0.1 K accuracy). A least-squares computer program[20] was used to fit the Mössbauer parameters and determine their standard deviations of statistical origin (given in parentheses). Isomer shift values (δ) are reported relative to iron foil at 300 K. Variable-temperature (2−300 K) dc magnetic susceptibility data were collected on powdered microcrystalline solids on a Cryogenics S600 SQUID magnetometer (complexes **1**·H_2O and **3**) and on a Quantum Design MPMS SQUID susceptometer (complex **2**·MeCN). Data were corrected with the standard procedure for the contribution of the sample holder and diamagnetism of the sample. Solid-state EPR spectra in the 4−300 K temperature range were recorded on a Varian ESR9 X-band spectrometer, equipped with an Oxford helium continuous-flow cryostat, a Hall probe, and a Hewlett-Packard frequency meter.

X-ray Crystallography. Crystals of **1**·4.4MeCN·H_2O, **2**·2MeCN, and **3**·2H_2O were sealed in capillaries filled with drops of the mother liquors and mounted on a Crystal Logic dual goniometer (complexes **1** and **3**) and a $P2_1$ Nicolet diffractometer (complex **2**). Complete crystal data and parameters for data collection for the three complexes are reported in Table 1. Intensity data were recorded using a $\theta-2\theta$ scan. Three standard reflections monitored every 97 reflections showed less that 3% variation and no decay. Lorentz, polarization, and Ψ-scan absorption (for **2**·2MeCN and **3**·2H_2O) corrections were applied using Crystal Logic software. The structures were solved by direct methods using SHELXS-86[21a] and refined by full-matrix least-squares techniques on F^2 with SHELXL-93.[21b]

Further crystallographic details are briefly as follows. Complex **1**·4.4MeCN·H_2O: $2\theta(\max) = 43°$ (Mo Kα radiation), scan speed = 1.5°/min, scan range = 2.1° + $\alpha_1\alpha_2$ separation, reflections collected/unique/used 10 810/10 253 ($R_{int} = 0.0694$)/10 250, 914 parameters refined, $(\Delta\rho)_{max}/(\Delta\rho)_{min} = 0.847/-0.649$ e/Å^3, $(\Delta/\sigma) = 0.304$. Complex **2**·2MeCN: $2\theta(\max) = 97.5°$ (Cu Kα radiation), scan speed = 1.5°/min, scan range = 2.9° + $\alpha_1\alpha_2$ separation, reflections collected/unique/used 7860/7370 ($R_{int} = 0.0403$)/7370, 964 parameters refined, $(\Delta\rho)_{max}/(\Delta\rho)_{min} = 0.944/-0.552$ e/Å^3, $(\Delta/\sigma) = 0.029$. Complex **3**·2H_2O: $2\theta(\max) = 48.5°$ (Mo Kα radiation), scan speed = 1.5°/min, scan range = 2.2° + $\alpha_1\alpha_2$ separation, reflections collected/unique/used 6765/6469 ($R_{int} = 0.0294$)/6292, 596 parameters refined, $(\Delta\rho)_{max}/(\Delta\rho)_{min} = 0.600/-0.339$ e/Å^3, $(\Delta/\sigma) = 0.008$.

For **1**·4.4MeCN·H_2O and **2**·2MeCN, all hydrogen atoms were introduced at calculated positions as riding on bonded atoms. All non-hydrogen atoms were refined anisotropically except the oxygens of the two perchlorate ions (**1**) and those of the solvent molecules (**1**, **2**) which were refined isotropically. For **3**·2H_2O, all hydrogen atoms were located by difference maps and refined isotropically, except those on C(26) and C(57), which were introduced at calculated positions as riding on bonded atoms. All non-hydrogen atoms were refined anisotropically, except those of the solvent water which were refined isotropically.

Results and Discussion

Syntheses. Previous investigations using 1,10-phenanthroline (phen) in iron(III) carboxylate chemistry led to the isolation of $[Fe_2O(O_2CPh)_2(phen)_4]Cl_2$,[12] $[Fe_3O_2(O_2CMe)_2(phen)_6](ClO_4)_3$,[13] and $Na[Fe_6O_4(OH)_2(ami)_4(phen)_8](NO_3)_9$,[14] where ami is the zwitterionic form of β-alanine. The first of these complexes contains the $[Fe_2(\mu\text{-}O)]^{4+}$ core, while the second consists of a bent Fe^{III}_3 line which can be described as two identical $[Fe_2(\mu\text{-}O)]^{4+}$ units with a common central Fe^{III} atom; in both complexes the carboxylate ligands are monodentate. The ring-shaped hexanuclear cation consists of two $[Fe_2(\mu\text{-}OH)(\mu\text{-}O_2CR)_2(phen)_2]^{2+}$ subunits, each linked to the two additional Fe^{III} atoms through two single μ-O^{2-} groups; thus, this complex contains the $[Fe_2(\mu\text{-}OH)(\mu\text{-}O_2$-

(20) Varret, F. *Proceedings of the International Conference on Mössbauer Effect Applications*; Indian National Science Academy: New Delhi, 1982.

(21) (a) Sheldrick, G. M. *SHELXS-86: Structure Solving Program*; University of Göttingen: Göttingen, Germany, 1986. (b) Sheldrick, G. M. *SHELXL-93: Crystal Structure Refinement Program*; University of Göttingen: Göttingen, Germany, 1993.

$CR)_2]^{2+}$ and $[Fe_2(\mu\text{-}O)]^{4+}$ cores. The syntheses of the dinuclear and trinuclear complexes both involved the 1:2 Fe^{III}/phen ratio.[12,13] We wondered whether 1:1 Fe^{III}/phen carboxylate clusters would be capable of existence, and thus, we employed the 1:1 reaction ratio. Complex $[Fe_4(OHO)(OH)_2(O_2CMe)_4(phen)_4](ClO_4)_3$ (**1**) was obtained using the 1:1.75:1 $Fe(ClO_4)_3 \cdot 6H_2O/NaO_2CMe \cdot 3H_2O$/phen ratio in MeCN. Its formation is summarized in eq 1, on the basis of the reasonable assumption that H_2O is the source of the OHO^{3-} and OH^- ions. The excess of $NaO_2CMe \cdot 3H_2O$ is beneficial to the preparation. Use of the stoichiometric amount of $NaO_2CMe \cdot 3H_2O$ (a 1:1:1 reaction ratio) does not give pure complex **1**; instead, a small amount of $[Fe_2O(O_2CMe)_2(phen)_4](ClO_4)_3$[11] precipitates from solution and this material has proven difficult to separate.

$$4Fe(ClO_4)_3 \cdot 6H_2O + 4NaO_2CMe \cdot 3H_2O + 4phen \xrightarrow[20\ ^\circ C]{MeCN} [Fe_4(OHO)(OH)_2(O_2CMe)_4(phen)_4](ClO_4)_3 + 4NaClO_4 + 5HClO_4 + 32H_2O \quad (1)$$

Since single-crystal X-ray crystallography revealed the existence of the new $[Fe_4(\mu_4\text{-}OHO)(\mu\text{-}OH)_2]^{7+}$ core in **1** (vide infra), we sought to prepare the benzoate analogue of **1**, i.e., complex $[Fe_4(OHO)(OH)_2(O_2CPh)_4(phen)_4](ClO_4)_3$. However, the $Fe(ClO_4)_3 \cdot 6H_2O/NaO_2CPh$/phen (1:1.75:1) reaction mixture in MeCN yielded the tetranuclear complex $[Fe_4O_2(O_2CPh)_7(phen)_2](ClO_4)$ (**2**) containing a "butterfly"-type $[Fe_4(\mu_3\text{-}O)_2]^{8+}$ core (vide infra). The formation of **2** is summarized in eq 2. The "excess" NaO_2CPh over that required for formation of the benzoate analogue of **1** was considered to be a possible reason for the isolation of **2**. When we sought to prevent formation of **2**, an $Fe(ClO_4)_3 \cdot 6H_2O/NaO_2CPh$/phen reaction ratio of 1:1:1 was employed. However, this reaction system gave a mixture of green-purple crystals of **2**·2MeCN (identified by unit cell determination) and a red-brown microcrystalline solid; the latter was formulated as $[Fe_2O(O_2CPh)_2(phen)_4](ClO_4)_2 \cdot 5H_2O$ on the basis of elemental analyses, and it presumably has a structure similar to that of $[Fe_2O(O_2CPh)_2(phen)_4]Cl_2 \cdot 7H_2O$.[12]

$$4Fe(ClO_4)_3 \cdot 6H_2O + 7NaO_2CPh + 2phen \xrightarrow[20\ ^\circ C]{MeCN} [Fe_4O_2(O_2CPh)_7(phen)_2](ClO_4) + 7NaClO_4 + 4HClO_4 + 22H_2O \quad (2)$$

Looking for an alternative method for preparing the benzoate analogue of **1**, we anticipated that complex **1** would be capable of $MeCO_2^-$ substitution on treatment with $PhCO_2H$. Such a reactivity pattern is consistent with the known acidities of the RCOOH molecules as reflected in the pK_a values (pK_a of $MeCO_2H = 4.75$, pK_a of $PhCO_2H = 4.19$), and the probable mechanism[22a] involves protonation of bound acetates by more acidic $PhCO_2H$ molecules, followed by their displacement by generated $PhCO_2^-$'s. Such ligand substitutions have been widely used in metal carboxylate cluster chemistry.[22] Unfortunately, we could not confirm this type of reactivity for **1**. Addition of $PhCO_2H$ in excess to **1** gave pure **2** in low yield according to eq 3. This represents a second route to complex **2** (method B in the Experimental Section). The precise means of formation of **2** from the $[Fe_4(\mu_4\text{-}OHO)(\mu\text{-}OH)_2]^{7+}$ precursor is undoubtedly complex, but it may be initiated by protonation of core OH^- and OHO^{3-} ions and $MeCO_2^-$ ions, facilitated by the relatively low pK_a value of $PhCO_2H$, triggering reorganization of the structure. We have found that addition of $NaClO_4$ in the reaction mixture assists precipitation of **2** in MeCN providing a higher yield route to this compound (method C).

Scheme 1

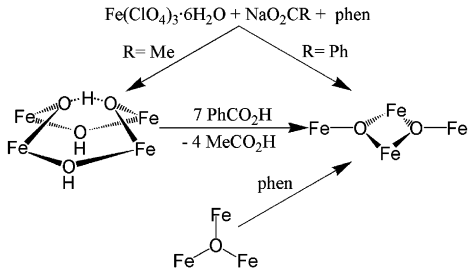

$$[Fe_4(OHO)(OH)_2(O_2CMe)_4(phen)_4](ClO_4)_3 + 7PhCO_2H \xrightarrow[20\ ^\circ C]{MeCN} [Fe_4O_2(O_2CPh)_7(phen)_2](ClO_4) + 4MeCO_2H + 2HClO_4 + 2phen + 2H_2O \quad (3)$$

Omitting the counterion from the reaction mixture does not greatly influence the structural identity of the product. The 1:1 reaction between basic iron(III) benzoate, "$Fe_3(OH)O(O_2CPh)_6(H_2O)_2$", and phen·$H_2O$ in MeCN yielded a brown-green solution from which $[Fe_4O_2(O_2CPh)_8(phen)_2]$ (**3**) was crystallized in low yield (~20%). Complex **3** is structurally analogous to **2** in that it also contains the "butterfly"-type $[Fe_4(\mu_3\text{-}O)_2]^{8+}$ core. However, an additional $PhCO_2^-$ had to be introduced to balance charges; this resulted in the replacement of the body−body benzoate bridge by two terminal monodentate benzoates (vide infra). Once the existence of **3** had been established, it was possible to design a more rational synthesis that gave this complex in a better yield (~40%). In this improved procedure (see Experimental Section), the exact stoichiometric Fe^{III}/phen was used according to eq 4.

For convenience, the preparations/transformations described above are summarized in Scheme 1.

$$4\text{"}Fe_3(OH)O(O_2CPh)_6(H_2O)_2\text{"} + 6phen \xrightarrow[20\ ^\circ C]{MeCN} 3[Fe_4O_2(O_2CPh)_8(phen)_2] + 10H_2O \quad (4)$$

Description of Structures. Selected interatomic distances and angles for complexes **1**·4.4MeCN·H_2O, **2**·2MeCN, and **3**·2H_2O are listed in Tables 2−4; ORTEP representations are presented in Figures 1−3. Complex **1**·4.4MeCN·H_2O crystallizes in monoclinic space group $P2/n$. Its structure consists of the tetranuclear $[Fe_4(OHO)(OH)_2(O_2CMe)_4$-

(22) (a) Vincent, J. B.; Christmas, C.; Chang, H.-R.; Li, Q.; Boyd, P. D. W.; Huffman, J. C.; Hendrickson, D. N.; Christou, G. C. *J. Am. Chem. Soc.* **1989**, *111*, 2086. (b) Christou, G. C.; Perlepes, S. P.; Libby, E.; Folting, K.; Huffman, J. C.; Webb, R. J.; Hendrickson, D. N. *Inorg. Chem.* **1990**, *29*, 3657.

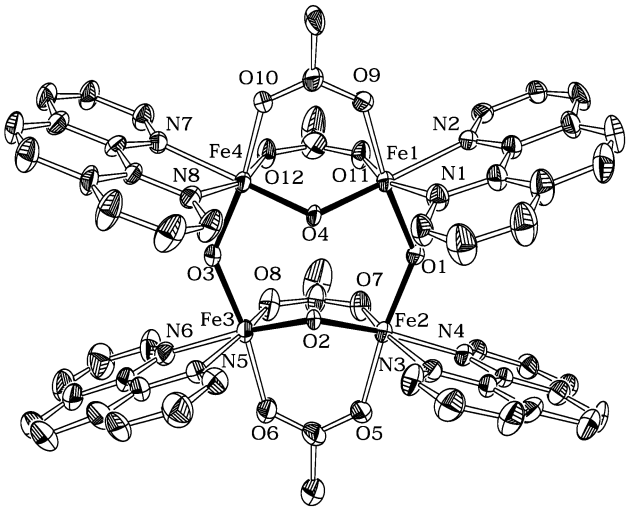

Figure 1. ORTEP representation of the cation of complex **1**·4.4MeCN·H_2O at the 30% probability level. The μ-OH^- oxygen atoms are O(1) and O(3), while atoms O(2) and O(4) belong to the OHO^{3-} group.

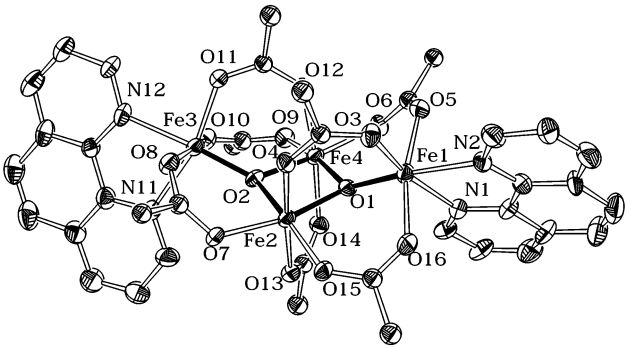

Figure 2. ORTEP representation of the tetranuclear cation of complex **2**·2MeCN at the 30% probability level. For clarity, only the ipso C atom of phenyl rings of the benzoate groups is included.

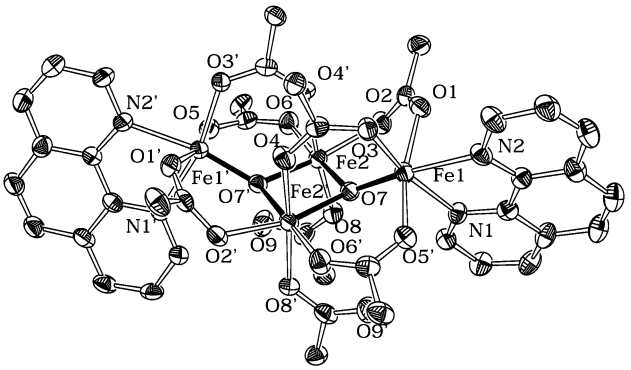

Figure 3. ORTEP representation of the tetranuclear molecule of complex **3**·2H_2O at the 30% probability level. For clarity, only the ipso C atom of phenyl rings of the benzoate groups is included. Primed and unprimed atoms are related by the crystallographic 2-fold axis.

$(phen)_4]^{3+}$ cation, three ClO_4^- anions, and solvate H_2O and MeCN molecules; the latter three will not be further discussed. The four Fe^{III} atoms lie at the corners of a rectangle and deviate from their best least-squares plane by only ~0.018 Å. Each of the Fe(1)/Fe(4) and Fe(2)/Fe(3) pairs is bridged by one O^{2-} group and two $MeCO_2^-$ ligands; the latter are in the familiar η^1:η^1:μ_2 mode. One single OH^- group (vide infra) bridges each of the Fe(1)/Fe(2) and Fe(3)/Fe(4) pairs. Fe···Fe separations bridged by three

Table 2. Selected Interatomic Distances (Å) and Angles (deg) for Complex **1**·4.4MeCN·H_2O

Fe(1)···Fe(2)	3.694(2)	Fe(2)−N(4)	2.164(9)
Fe(3)···Fe(4)	3.687(2)	Fe(3)−O(2)	1.876(7)
Fe(1)···Fe(4)	3.261(2)	Fe(3)−O(3)	1.984(7)
Fe(2)···Fe(3)	3.250(2)	Fe(3)−O(6)	2.028(9)
Fe(1)−O(4)	1.883(6)	Fe(3)−O(8)	2.005(10)
Fe(1)−O(1)	1.997(7)	Fe(3)−N(5)	2.136(11)
Fe(1)−O(9)	2.038(8)	Fe(3)−N(6)	2.186(11)
Fe(1)−O(11)	1.998(8)	Fe(4)−O(4)	1.869(6)
Fe(1)−N(1)	2.138(10)	Fe(4)−O(3)	2.002(7)
Fe(1)−N(2)	2.186(9)	Fe(4)−O(10)	2.045(8)
Fe(2)−O(2)	1.881(7)	Fe(4)−O(12)	1.991(8)
Fe(2)−O(1)	1.997(7)	Fe(4)−N(7)	2.180(9)
Fe(2)−O(5)	2.035(8)	Fe(4)−N(8)	2.172(9)
Fe(2)−O(7)	2.014(9)	O(2)···O(4)	2.525(9)
Fe(2)−N(3)	2.148(9)		

O(1)−Fe(1)−O(4)	94.1(3)	O(2)−Fe(3)−N(6)	171.1(4)
O(1)−Fe(1)−O(9)	173.5(3)	O(3)−Fe(3)−O(6)	172.2(3)
O(1)−Fe(1)−O(11)	91.9(3)	O(3)−Fe(3)−O(8)	92.9(4)
O(1)−Fe(1)−N(1)	88.9(4)	O(3)−Fe(3)−N(5)	90.1(3)
O(1)−Fe(1)−N(2)	89.5(3)	O(3)−Fe(3)−N(6)	89.3(3)
O(4)−Fe(1)−O(9)	91.4(3)	O(6)−Fe(3)−O(8)	88.8(4)
O(4)−Fe(1)−O(11)	99.7(3)	O(6)−Fe(3)−N(5)	86.1(4)
O(4)−Fe(1)−N(1)	97.7(3)	O(6)−Fe(3)−N(6)	83.1(4)
O(4)−Fe(1)−N(2)	172.8(4)	O(8)−Fe(3)−N(5)	163.1(4)
O(9)−Fe(1)−O(11)	90.7(4)	O(8)−Fe(3)−N(6)	88.1(4)
O(9)−Fe(1)−N(1)	86.8(4)	N(5)−Fe(3)−N(6)	75.3(5)
O(9)−Fe(1)−N(2)	84.7(3)	O(3)−Fe(4)−O(4)	94.2(3)
O(11)−Fe(1)−N(1)	162.4(4)	O(3)−Fe(4)−O(10)	172.5(3)
O(11)−Fe(1)−N(2)	86.3(4)	O(3)−Fe(4)−O(12)	92.5(4)
N(1)−Fe(1)−N(2)	76.1(4)	O(3)−Fe(4)−N(7)	88.7(3)
O(1)−Fe(2)−O(2)	94.0(3)	O(3)−Fe(4)−N(8)	90.7(3)
O(1)−Fe(2)−O(5)	172.9(3)	O(4)−Fe(4)−O(10)	92.0(3)
O(1)−Fe(2)−O(7)	91.3(4)	O(4)−Fe(4)−O(12)	99.5(3)
O(1)−Fe(2)−N(3)	90.5(3)	O(4)−Fe(4)−N(7)	172.6(3)
O(1)−Fe(2)−N(4)	89.2(3)	O(4)−Fe(4)−N(8)	97.7(3)
O(2)−Fe(2)−O(5)	92.9(3)	O(10)−Fe(4)−O(12)	90.7(4)
O(2)−Fe(2)−O(7)	99.5(3)	O(10)−Fe(4)−N(7)	84.7(3)
O(2)−Fe(2)−N(3)	96.5(3)	O(10)−Fe(4)−N(8)	84.2(4)
O(2)−Fe(2)−N(4)	171.4(3)	O(12)−Fe(4)−N(7)	87.2(3)
O(5)−Fe(2)−O(7)	88.9(4)	O(12)−Fe(4)−N(8)	162.2(3)
O(5)−Fe(2)−N(3)	87.3(4)	N(7)−Fe(4)−N(8)	75.4(3)
O(5)−Fe(2)−N(4)	83.8(3)	Fe(1)−O(1)−Fe(2)	135.3(4)
O(7)−Fe(2)−N(3)	163.7(4)	Fe(3)−O(3)−Fe(4)	135.3(4)
O(7)−Fe(2)−N(4)	88.4(4)	Fe(2)−O(2)−Fe(4)	119.8(4)
N(3)−Fe(2)−N(4)	75.4(4)	Fe(1)−O(4)−Fe(4)	120.7(4)
O(2)−Fe(3)−O(3)	93.8(3)	C(53)−O(7)−Fe(2)	132.6(8)
O(2)−Fe(3)−O(6)	93.4(3)	C(55)−O(10)−Fe(4)	131.0(8)
O(2)−Fe(3)−O(8)	100.1(3)	O(5)−C(51)−O(6)	125.9(12)
O(2)−Fe(3)−N(5)	96.3(4)	O(7)−C(53)−O(8)	125.3(12)

ligands are significantly shorter (~3.25 Å) than those bridged by the single μ-OH^- ion (~3.69 Å). A chelating phen molecule completes a distorted octahedral coordination at each metal center. Atoms O(2) and O(4) are 0.74 and 0.73 Å, respectively, above the best Fe_4 plane, while atoms O(1) and O(3) are both below this plane by 0.21 and 0.18 Å, respectively.

As stated in the Experimental Section, the H atoms of the cluster were not crystallographically located. Given the fact that the four metal centers are clearly high-spin (as evidenced by Fe−O and Fe−N bond lengths,[8−16] and by ^{57}Fe-Mössbauer spectroscopy—see below) and the crystallographically established presence of three ClO_4^- ions, charge considerations require that three core O atoms should be formally protonated. Core O atoms O(1) and O(3) are protonated as evidenced by (i) their bond distances to Fe^{III}atoms [mean 1.995(7) Å], which are typical of Fe^{III}−(μ-$O_{hydroxo}$)

bonds,[2c,d,14,24] and (ii) the close approach of two lattice MeCN molecules to H-bonding distances [O(1)···N(10) = 3.063(3), O(3)···N(9) = 3.013(3) Å]. The Fe−O(2, 4) bond distances are markedly shorter than the Fe−O(1, 3) distances, suggesting a different nature for O(2) and O(4). However, the Fe−O(2, 4) bond lengths fall outside the upper end of the range reported (1.76−1.82 Å) for complexes containing the $[Fe_2(\mu\text{-}O)(\mu\text{-}O_2CR)_2]^{2+}$ unit[8a,24a,25] and the lower limit of the range reported (1.93−1.98 Å) for complexes containing the $[Fe_2(\mu\text{-}OH)(\mu\text{-}O_2CR)_2]^{3+}$ unit.[2c,d,14,24b,c] Furthermore, we note that the bridging unit atoms O(2) and O(4) are not within H-bonding distance of any other ligand or lattice species, but their distance [2.529(9) Å] is such that the presence of a proton between them is possible.[26,27] The presence of such a proton would confer partial hydroxo character to the O(2), O(4) "oxo" groups and would be expected to result in elongation of the $Fe-O_{oxo}$ distances.[25] Consistent with this assignment, the Fe(1)···Fe(4) and Fe(2)···Fe(3) distances [3.261(2), 3.250(2) Å] are intermediate between those found in complexes containing the $[Fe_2(\mu\text{-}OH)(\mu\text{-}O_2CR)_2]^{3+}$ (∼3.45 Å)[2c,d,14,24a,b] and $[Fe_2(\mu\text{-}O)(\mu\text{-}O_2CR)_2]^{2+}$ (3.06−3.18 Å) units.[8a,24a,25] Finally, the trans influence expected[24a,25a,28] for a pure $\mu\text{-}O^{2-}$ group is also reduced, resulting in a *slight* elongation of the Fe−N bonds in trans positions (compared with those in cis positions) and suggesting that O(2) and O(4) are not $\mu\text{-}O^{2-}$ groups. For example the Fe(1)−N(2) bond trans to O(4) has a length of 2.186(9) Å, while the length of the corresponding cis bond [Fe(1)−N(1)] is 2.138(10) Å. On the basis of the above strong crystallographic evidence, we are confident in the assignment of the new $[Fe_4(\mu_4\text{-}OHO)(\mu\text{-}OH)_2]^{7+}$ core in **1**. It should be mentioned at this point that Fe^{III} clusters in which the hydroxo[2a,c,d,14,29] or OHO^{3-} [26] hydrogens were not crystallographically located are by no means rare. Further support to this assignment arises from IR spectroscopy (vide infra).

An alternative description of the structure is also useful: the cation of **1** may be considered as consisting of two $\{Fe_2(\mu\text{-}O)(\mu\text{-}O_2CR)_2(phen)_2\}^{2+}$ fragments triply bridged by two $\mu\text{-}OH^-$ groups and one proton. An analogous dinuclear fragment, with bpy in place of phen, has been structurally characterized in the discrete dinuclear complex $[Fe_2O(O_2CR)_2(bpy)_2Cl_2]$,[8a] which contains a terminally coordinated Cl^- at each Fe^{III}. Tetranuclear complexes containing Fe^{III} atoms bridged solely by one $\mu\text{-}OH^-$ group (complex **1** can be regarded as containing Fe^{III} atoms bridged by a single $\mu\text{-}OH^-$ group, if we ignore the OHO^{3-} bridging group) are also known;[30] these complexes contain the adamantane-like cores $[Fe_4(\mu\text{-}O)_2(\mu\text{-}OH)_4]^{4+}$ [30a] and $[Fe^4(\mu\text{-}O)_2(\mu\text{-}OH)_2(\mu\text{-}OR)_2]^{4+}$.[30b, c] Examples of Fe^{III} clusters containing the $\mu_4\text{-}OHO^{3-}$ group are known;[26,31] they are all tetranuclear. A diagram of the $[Fe_4(\mu\text{-}OHO^{3-})]^{9+}$ unit, defining its metrical parameters, is shown in Scheme 2. The O···O distances (a) in the reported complexes are in the range 2.394(1)-2.426(4) Å, slightly shorter than (a) in **1** [2.525(9) Å]. The Fe···Fe distances through the "end-on" (b, b′) and to "end-to-end" (c, c′) parts of $\mu_4\text{-}OHO^{3-}$ are in the ranges 3.397(1)−3.474(1) and 3.675(1)−3.755(1) Å, respectively; the corresponding average values in **1** are 3.255(2) and 3.691(2) Å. The shorter b, b′ distances in **1** reflect the presence of two triatomic exogeneous bridges (two $MeCO_2^-$) in the present complex; there is only one triatomic bridge (RCO_2^-, CO_3^-) connecting the Fe^{III} atoms that are bridged by the "end-on" parts of OHO^{3-} in the literature examples.[26,31] This structural difference results in smaller values for the angles α, α′ in **1** [119.8(4), 120.7(4)°] compared to the reported complexes [136.4(3)−138.4(3)°]. Another difference between **1** and literature examples[26,31] is the fact that in the latter the OHO^{3-} moiety is coplanar with the Fe^{III} atoms; this makes our cation the first example of an out-of-plane $\mu_4\text{-}OHO^{3-}$ group in Fe^{III} cluster chemistry and the third in general. The two reported[32] examples were the $Mn^{II}Mn^{III}$ complexes $(Ba,Ca)_2[Mn_4(OHO)(O_2CMe)_2L_2]$ and $(Ca)_2[Mn_4(OHO)(O_2CMe)_2L_2]$, where L is the pentaanion of 1,3-diamino-2-hydroxypropane-*N*,*N*,*N*′,*N*′-tetraacetic acid. The $\mu_4\text{-}OHO^{3-}$ ligand is currently of great bioinorganic interest, because it has been proposed to exist,[32a] either in an in-plane or in an out-of-plane fashion, in the oxygen-evolving Mn_4 complex during the S_1, S_2 states. Recently, crystallographic

Scheme 2

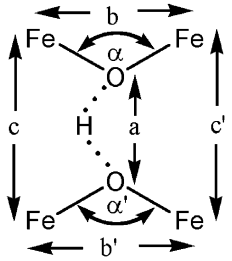

(23) (a) Grant, C. M.; Knapp, M. J.; Streib, W. E.; Huffman, J. C.; Hendrickson, D. N.; Christou, G. C. *Inorg. Chem.* **1998**, *37*, 6065. (b) Satcher, J. H., Jr.; Olmstead, M. M.; Droege, M. W.; Parkin, S. R.; Coll, B. C.; May, L.; Balch, A. L. *Inorg. Chem.* **1998**, *37*, 6751.
(24) (a) Kurtz, D. M., Jr. *Chem. Rev.* **1990**, *90*, 585. (b) Armstrong, W. H.; Lippard, S. J. *J. Am. Chem. Soc.* **1984**, *106*, 4632. (c) Vankai, V. A.; Newton, M. G.; Kurtz, D. M., Jr. *Inorg. Chem.* **1992**, *31*, 341. (d) Kitajima, N.; Amagai, H.; Tamura, N.; Ito, M.; Moro-oka, Y.; Heerwegh, K.; Penicaud, A.; Mathur, R.; Reed, C. A.; Boyd, P. D. W. *Inorg. Chem.* **1993**, *32*, 3583. (e) Micklitz, W.; Lippard, S. J. *Inorg. Chem.* **1988**, *27*, 3067.
(25) (a) Wu, F.-J.; Kurtz, D. M., Jr.; Hagen, K. S.; Nyman, P. D.; Debrunner, P. G.; Vankai, V. A. *Inorg. Chem.* **1990**, *29*, 5174. (b) Gorun, S. M.; Lippard, S. J. *Inorg. Chem.* **1991**, *30*, 1625.
(26) Jameson, D. L.; Xie, C.-L.; Hendrickson, D. N.; Potenza, J. A.; Sugar, H. G. *J. Am. Chem. Soc.* **1987**, *109*, 740.
(27) Braga, D.; Grepioni, F.; Novoa, J. J. *Chem. Commun.* **1998**, 1959.
(28) Plakatouras, J. C.; Bakas, T.; Huffman, C. J.; Huffman, J. C.; Papaefthymiou, V.; Perlepes, S. P. *J. Chem. Soc., Dalton Trans.* **1994**, 2737.
(29) (a) Gorun, S. M.; Papaefthymiou, G. C.; Frankel, R. B.; Lippard, S. J. *J. Am. Chem. Soc.* **1987**, *109*, 3337. (b) Parsons, S.; Solan, G. A.; Winpenny, R. E. P. *J. Chem. Soc., Chem. Commun.* **1995**, 1987.
(30) (a) Drüeke, S.; Wieghardt, K.; Nuber, B.; Weiss, J.; Bominaar, E. L.; Sawaryn, A.; Winkler, H.; Trautwein, A. X. *Inorg. Chem.* **1989**, *28*, 4477. (b) Murch, B. P.; Bradley, F. C.; Boyle, P. D.; Papaefthymiou, V.; Que, L., Jr. *J. Am. Chem. Soc.* **1987**, *109*, 7993. (c) Sessler, J. L.; Sibert, J. W.; Burrell, A. K.; Lynch, V.; Markert, J. T.; Wooten, C. L. *Inorg. Chem.* **1993**, *32*, 4277.
(31) (a) Tanase, T.; Inagaki, Y.; Yamada, Y.; Kato, M.; Ota, E.; Yamazaki, M.; Sato, M.; Mori, W.; Yamaguchi, K.; Mikuriya, M.; Takahashi, M.; Takeda, M.; Kinoshita I.; Yano, S. *J. Chem. Soc., Dalton Trans.* **1998**, 713. (b) Tanase, T.; Inoue, C.; Ota, E.; Yano, S.; Takahashi, M.; Takeda, M. *Inorg. Chim. Acta* **2000**, *297*, 18.
(32) (a) Stibrany, R. T.; Gorun, S. M. *Angew. Chem., Int. Ed. Engl.* **1990**, *29*, 1156. (b) Gorun, S. M.; Stibrany, R. T.; Lillo, A. *Inorg. Chem.* **1998**, *37*, 836.

Table 3. Selected Interatomic Distances (Å) and Angles (deg) for Complex **2**·2MeCN

Fe(1)···Fe(2)	3.302(1)	Fe(2)−O(7)	2.025(6)
Fe(1)···Fe(4)	3.458(1)	Fe(2)−O(13)	2.047(6)
Fe(1)···Fe(3)	5.880(2)	Fe(2)−O(15)	2.000(6)
Fe(2)···Fe(3)	3.472(2)	Fe(3)−O(2)	1.807(6)
Fe(2)···Fe(4)	2.879(2)	Fe(3)−O(8)	2.001(7)
Fe(3)···Fe(4)	3.296(2)	Fe(3)−O(10)	2.032(7)
Fe(1)−O(1)	1.819(6)	Fe(3)−O(11)	1.972(7)
Fe(1)−O(3)	1.978(6)	Fe(3)−N(11)	2.160(9)
Fe(1)−O(5)	2.036(6)	Fe(3)−N(12)	2.162(8)
Fe(1)−O(16)	2.015(7)	Fe(4)−O(1)	1.934(6)
Fe(1)−N(1)	2.136(9)	Fe(4)−O(2)	1.916(6)
Fe(1)−N(2)	2.169(8)	Fe(4)−O(6)	2.014(6)
Fe(2)−O(1)	1.925(6)	Fe(4)−O(9)	2.027(6)
Fe(2)−O(2)	1.959(6)	Fe(4)−O(12)	2.059(6)
Fe(2)−O(4)	2.043(6)	Fe(4)−O(14)	2.062(6)
O(1)−Fe(1)−O(3)	96.7(3)	O(2)−Fe(3)−N(11)	99.1(3)
O(1)−Fe(1)−O(5)	93.4(3)	O(2)−Fe(3)−N(12)	174.5(3)
O(1)−Fe(1)−O(16)	94.6(3)	O(8)−Fe(3)−O(10)	166.4(3)
O(1)−Fe(1)−N(1)	97.7(3)	O(8)−Fe(3)−O(11)	94.7(3)
O(1)−Fe(1)−N(2)	174.3(3)	O(8)−Fe(3)−N(11)	85.7(3)
O(3)−Fe(1)−O(5)	94.3(3)	O(8)−Fe(3)−N(12)	88.6(3)
O(3)−Fe(1)−O(16)	94.2(3)	O(10)−Fe(3)−O(11)	95.7(3)
O(3)−Fe(1)−N(1)	165.6(3)	O(10)−Fe(3)−N(11)	81.9(3)
O(3)−Fe(1)−N(2)	89.0(3)	O(10)−Fe(3)−N(12)	83.0(3)
O(5)−Fe(1)−O(16)	167.5(3)	O(11)−Fe(3)−N(11)	164.5(3)
O(5)−Fe(1)−N(1)	85.1(3)	O(11)−Fe(3)−N(12)	88.4(3)
O(5)−Fe(1)−N(2)	86.9(3)	N(11)−Fe(3)−N(12)	76.1(3)
O(16)−Fe(1)−N(1)	84.4(3)	O(1)−Fe(4)−O(2)	83.8(2)
O(16)−Fe(1)−N(2)	84.1(3)	O(1)−Fe(4)−O(6)	89.9(3)
N(1)−Fe(1)−N(2)	76.6(3)	O(1)−Fe(4)−O(9)	168.9(3)
O(1)−Fe(2)−O(2)	82.9(2)	O(1)−Fe(4)−O(12)	97.5(3)
O(1)−Fe(2)−O(4)	88.3(2)	O(1)−Fe(4)−O(14)	85.5(3)
O(1)−Fe(2)−O(7)	167.6(3)	O(2)−Fe(4)−O(6)	167.9(3)
O(1)−Fe(2)−O(13)	90.3(3)	O(2)−Fe(4)−O(9)	96.2(3)
O(1)−Fe(2)−O(15)	96.0(3)	O(2)−Fe(4)−O(12)	87.8(3)
O(2)−Fe(2)−O(4)	97.5(2)	O(2)−Fe(4)−O(14)	87.4(3)
O(2)−Fe(2)−O(7)	89.0(3)	O(6)−Fe(4)−O(9)	92.0(3)
O(2)−Fe(2)−O(13)	84.5(2)	O(6)−Fe(4)−O(12)	82.8(3)
O(2)−Fe(2)−O(15)	170.8(3)	O(6)−Fe(4)−O(14)	102.5(3)
O(4)−Fe(2)−O(7)	83.5(3)	O(9)−Fe(4)−O(12)	93.6(3)
O(4)−Fe(2)−O(13)	177.4(3)	O(9)−Fe(4)−O(14)	83.5(3)
O(4)−Fe(2)−O(15)	91.6(3)	O(12)−Fe(4)−O(14)	174.1(3)
O(7)−Fe(2)−O(13)	98.2(3)	Fe(1)−O(1)−Fe(2)	123.7(3)
O(7)−Fe(2)−O(15)	93.6(3)	Fe(1)−O(1)−Fe(4)	134.2(3)
O(13)−Fe(2)−O(15)	86.4(3)	Fe(2)−O(1)−Fe(4)	96.5(3)
O(2)−Fe(3)−O(8)	93.8(3)	Fe(2)−O(2)−Fe(4)	96.0(2)
O(2)−Fe(3)−O(10)	93.7(3)	Fe(2)−O(2)−Fe(3)	134.3(3)
O(2)−Fe(3)−O(11)	96.3(3)	Fe(3)−O(2)−Fe(4)	124.5(3)

data have begun to become available on the topological arrangement of the Mn ions of this important biological system;[34] however, the oxygen-based ligands of the metal ions could not be located at the available 3.8 Å resolution. Examples in which the OHO^{3-} group behaves as μ_2[35] or μ_5[32b] ligand are also known.

Complex **2**·2MeCN crystallizes in the monoclinic space group $P2_1/n$. Its cation contains a $[Fe_4(\mu_3\text{-}O)_2]^{8+}$ core comprising four Fe^{III} atoms with a "butterfly" disposition and a μ_3-O^{2-} ion bridging each Fe_3 "wing". Ions Fe(2) and Fe(4) occupy the "hinge" or "body" sites, and Fe(1) and Fe(3) occupy the "wing-tip" sites. Both oxide ions, O(1) and O(2), lie slightly above their respective Fe_3 planes by 0.25 and 0.24 Å, respectively, with sum of angles of 354.4 and 354.8°, respectively. The dihedral angle between the two Fe(3) planes is 147.6°. Thus, the core can be considered as two edge-sharing Fe_3O triangular units with the oxygen atoms above their Fe_3 planes (type **I** in the Introduction). Peripheral ligation is provided by seven $PhCO_2^-$ and two phen chelate groups, the former in their common *syn*,*syn*-bridging modes, and the latter attached to the wing-tip Fe^{III} centers, Fe(1) and Fe(3). The body/wing-tip Fe_2 pairs are bridged by six μ_2-carboxylate groups, while a seventh carboxylate bridges the two "hinge" ions, Fe(2) and Fe(4). The metals are all octahedrally coordinated, their chromophores being Fe(1, 3)N_2O_4 and Fe(2, 4)O_6, and the entire cation has a virtual C_2 symmetry. The Fe···Fe separations fall into four types. The body/body separation, Fe(2)···Fe(4), is short (2.879(2) Å) because these metal ions are bridged by two oxides. The wing-tip/body distances (all Fe^{III} atoms involved are bridged by a single oxide) separate into two types, those bridged by one $PhCO_2^-$ group (Fe(1)···Fe(4), 3.458(1) Å; Fe(2)···Fe(3), 3.472(2) Å) and those bridged by two (Fe(1)···Fe(2), 3.302(1) Å; Fe(3)···Fe(4), 3.296(2) Å). Finally, the wing-tip/wing-tip separation (Fe(1)···Fe(3), 5.880(2) Å) is the longest as expected. The "body"-Fe to μ_3-O distances are in the range 1.916(6)−1.959(6) Å (average 1.933 Å), whereas the "wing-tip"-Fe to μ_3-O distances are clearly shorter (average 1.813 Å). This asymmetry is also reflected in the bond angles at the triply bonding oxide atoms: the Fe(2)−O(1)−Fe(4) and Fe(2)−O(2)−Fe(4) angles (96.5(3) and 96.0(2)°, respectively) are much smaller than the other Fe−O−Fe angles (123.7(3)−134.3(3)°).

Table 4. Selected Interatomic Distances (Å) and Angles (deg) for Complex **3**·2H_2O[a]

Fe(1)···Fe(2)	3.456(1)	Fe(1)−N(1)	2.152(5)
Fe(1)···Fe(2)	3.275(1)	Fe(1)−N(2)	2.203(5)
Fe(2)···Fe(2)	2.912(1)	Fe(2)−O(2)	2.042(5)
Fe(1)···Fe(1)	5.780(2)	Fe(2)−O(4)	2.120(4)
Fe(1)−O(1)	2.059(5)	Fe(2)−O(6)	2.036(5)
Fe(1)−O(3)	1.998(4)	Fe(2)−O(7)	1.961(4)
Fe(1)−O(5)	2.051(5)	Fe(2)−O(7)	1.931(4)
Fe(1)−O(7)	1.821(4)	Fe(2)−O(8)	2.004(4)
O(1)−Fe(1)−O(3)	89.1(2)	O(2)−Fe(2)−O(7)	90.1(2)
O(1)−Fe(1)−O(5)	166.1(2)	O(2)−Fe(2)−O(7)	165.5(2)
O(1)−Fe(1)−O(7)	96.1(2)	O(2)−Fe(2)−O(8)	93.2(2)
O(1)−Fe(1)−N(1)	90.4(2)	O(4)−Fe(2)−O(6)	84.1(2)
O(1)−Fe(1)−N(2)	81.6(2)	O(4)−Fe(2)−O(7)	93.1(2)
O(3)−Fe(1)−O(5)	91.1(2)	O(4)−Fe(2)−O(7)	87.3(2)
O(3)−Fe(1)−O(7)	99.7(2)	O(4)−Fe(2)−O(8)	170.6(2)
O(3)−Fe(1)−N(1)	166.1(2)	O(6)−Fe(2)−O(7)	176.4(2)
O(3)−Fe(1)−N(2)	90.3(2)	O(6)−Fe(2)−O(7)	99.2(2)
O(5)−Fe(1)−O(7)	97.6(2)	O(6)−Fe(2)−O(8)	88.7(2)
O(5)−Fe(1)−N(1)	86.1(2)	O(7)−Fe(2)−O(7)	83.0(2)
O(5)−Fe(1)−N(2)	84.5(2)	O(7)−Fe(2)−O(8)	93.8(2)
O(7)−Fe(1)−N(1)	94.2(2)	O(7)−Fe(2)−O(8)	99.9(2)
O(7)−Fe(1)−N(2)	169.7(2)	Fe(1)−O(7)−Fe(2)	132.1(2)
N(1)−Fe(1)−N(2)	75.9(2)	Fe(1)−O(7)−Fe(2)	121.6(2)
O(2)−Fe(2)−O(4)	80.3(2)	Fe(2)−O(7)−Fe(2)	96.9(2)
O(2)−Fe(2)−O(6)	87.1(2)		

[a] Primed atoms are related by the symmetry operation 0.5 − *x*, *y*, 1 − *z* to their unprimed partner.

Complex **3**·2H_2O crystallizes in the monoclinic space group $I2/a$ and displays crystallographically imposed C_2 symmetry. The tetranuclear molecule contains a "butterfly"

(33) Proserpio, D. M.; Hoffmann, R.; Dismukes, G. C. *J. Am. Chem. Soc.* **1992**, *114*, 4374.
(34) Zouni, A.; Witt, H.-T.; Kern, J.; Fromme, P.; Krauss, N.; Saenger, W.; Orth, P. *Nature* **2001**, *409*, 739.
(35) Rapta, M.; Kamaras, P.; Jameson, G. B. *J. Am. Chem. Soc.* **1995**, *117*, 12865.

Table 5. Comparison of Selected Structural Parameters (Å, deg) for **2**, **3,** and Representative Iron(III) Carboxylate "Butterfly" Complexes Possessing the $[Fe_4(\mu_3\text{-}O)_2]^{8+}$ Core[a,b]

param	**2**[c]	**3**	**A**[c,d]	**B**[e]	**C**[c,f]	**D**[c,g]	**E**[h]
$Fe_b\cdots Fe_b$	2.879(2)	2.912(1)	2.829(4)	2.855(4)	2.843(2)	2.897(1)	2.878(3)
$Fe_b\cdots Fe_w$[i]	3.299(2)	3.275(1)	3.328(2)	3.306(4)	3.323(2)	n.r.	3.316(2)
$Fe_b\cdots Fe_w$[j]	3.465(2)	3.456(1)	3.494(3)	3.439(4)	3.470(2)	n.r.	3.462(2)
Fe_b-O_t[i]	1.920(6)	1.931(4)	1.906(7)	1.926(5)	1.913(5)	1.924(1)	1.907(7)
Fe_b-O_t[j]	1.946(5)	1.961(4)	1.961(8)	1.947(5)	1.948(5)	1.950(1)	1.945(7)
Fe_w-O_t	1.813(6)	1.821(4)	1.836(8)	1.819(5)	1.844(5)	1.855(1)	1.861(7)
$Fe_b-O_t-Fe_b$	96.3(3)	96.9(2)	94.0(3)	95.0(2)	94.8(2)	96.8(1)	96.7(3)
$Fe_b-O_t-Fe_w$[i]	124.1(3)	121.6(2)	125.5(5)	123.9(3)	124.3(5)	123.6(1)	123.2(4)
$Fe_b-O_t-Fe_w$[j]	134.2(3)	132.1(2)	133.8(5)	131.9(3)	132.4(3)	130.2(1)	130.9(4)
θ[k]	147.6	144.3	n.r.	139.6	n.r.	157.6	n.r.

[a] Quoted esd's for averaged values are the esd's of the individual values. [b] Subscripts: b = body, w = wingtip, t = triply bridging. [c] Averaged values using C_2 virtual symmetry. [d] Complex **A** is $(Et_4N)[Fe_4O_2(O_2CPh)_2(H_2B(pz)_2)_2]$. [e] Complex **B** is $[Fe_4O_2(O_2CMe)_7(bpy)_2](ClO_4)$. [f] Complex **C** is $(NBu_4n)[Fe_4O_2(O_2CMe)_7(pic)_2]$. [g] Complex **D** is $[Fe_4O_2Cl_2(O_2CMe)_6(3\text{-}Mepy)_4]$. [h] Complex **E** is $[Fe_4O_2Cl_2(O_2CMe)_6(py)_4]$. [i] For metal ions bridged by two RCO_2^- groups. [j] For metal ions bridged by one RCO_2^- group. [k] Dihedral angle between the Fe_3 planes. n.r. = not reported.

$[Fe_4(\mu_3\text{-}O)_2]^{8+}$ core very similar to that in the anion of **2**. The only essential structural difference between the two clusters is that the $PhCO_2^-$ group which bridges the body Fe^{III} sites in **2** has been replaced by two terminal, monodentate benzoate ligands in **3**, one coordinated to each of the two body metal ions. The unligated benzoate oxygen atom O(9) is hydrogen-bonded to the lattice H_2O molecule, with an $O_{water}\cdots O(9)$ distance of 2.88 Å. The dihedral angle between the Fe(1)Fe(2)Fe(2′) and Fe(1′)Fe(2)Fe(2′) planes is 144.3°. Most structural trends in **3** are similar to those seen in complex **2**; obviously, the replacement of the seventh bridging $PhCO_2^-$ by two monodentate $PhCO_2^-$ groups has little structural effect.

Complexes **2** and **3** join a small family of structurally characterized tetranuclear Fe^{III} clusters containing the "butterfly"-type $[Fe_4(\mu_3\text{-}O)_2]^{8+}$ core (**I**).[9a−e,15] Gorun and Lippard have carried out detailed analyses of the $[Fe_4(\mu_3\text{-}O)_2]^{8+}$ core geometries in both the planar and "butterfly"structural types by defining diagnostic interatomic distances and bond angles within this core.[16b] A careful comparison of these structural parameters for **2**, **3,** and the other members of the iron(III) "butterfly" family[9a−e,15] reveals a remarkable structural similarity of their cores. In Table 5 are compared selected structural parameters for **2**, **3**, and the representative iron(III) carboxylate "butterflies" $(Et_4N)[Fe_4O_2(O_2CPh)_2(H_2B(pz)_2)_2]$ (**A**, $H_2B(pz)_2^-$ = dihydrobis(1-pyrazolyl)borate),[15a] $[Fe_4O_2(O_2CMe)_7(bpy)_2](ClO_4)$ (**B**),[9a] $(NBu_4^n)[Fe_4O_2(O_2CMe)_7(pic)_2]$ (**C**, pic^- = picolinate),[9e] $[Fe_4O_2Cl_2(O_2CMe)_6(3\text{-}Mepy)_4]$ (**D**, 3-Mepy = 3-methylpyridine),[15c] and $[Fe_4O_2Cl_2(O_2CMe)_6(py)_4]$ (**E**, py = pyridine).[15d] Detailed comparisons for some of the previously reported $[Fe_4O_2]^{8+}$ complexes may be found elsewhere.[9a,15d,16b]

A final point of interest is that the $[M_4(\mu_3\text{-}O)_2]^{8+}$ (M = 3d metal) "butterfly" type core is known in vanadium(III),[36] chromium(III),[37] chromium(III)−iron(III)[38] mixed-metal, and manganese(III)[22a,39] carboxylate chemistry.

IR Spectroscopy. Further support to the structural assignment of **1** as a complex containing OH^- and OHO^{3-} groups (vide supra) comes from FT-IR spectroscopy. Two medium broad bands observed in the spectrum of the fully desolvated compound **1**, i.e., the form without MeCN and H_2O solvate molecules, at ∼3580 and 3070 cm^{-1} are assigned to the O−H stretching mode of the bridging OH^- and OHO^{3-} groups, respectively[24b,d,e,29a,40] Two broad peaks are observed upon deuteration, i.e., in the spectrum of $[Fe_4(ODO)(OD)_2(O_2CMe)_4(phen)_4](ClO_4)_3$ (**1a**): one centered at ∼2630 and a second at ∼2250 cm^{-1}. Considering that deuteration results in an isotropic red shift of $\sim 2^{1/2}$, these bands are assigned[24b] to the O−D stretching modes of the OD^- and ODO^{3-} groups, respectively. Of particular diagnostic significance in the low-frequency region is the medium peak at 870 cm^{-1}, which disappears in the spectrum upon deuteration; a new peak at 640 cm^{-1} appears in the spectrum of **1a**. Therefore, the 870 cm^{-1} band is assigned to the bridging OH^- deformation mode.[24d,40]

Bands of phen in the 1600−1400 cm^{-1}, attributed to ring stretching vibrations, shift to higher frequencies upon chelation[4141] in **1**−**3**. Similar shifts occur for the bands between 1250 and 1100 cm^{-1}, while those between 1050 and 700 cm^{-1} shift to lower frequencies with splitting of the band at ∼850 cm^{-1} (an out-of-plane C−H deformation).[41]

The strong bands at 1570 (**1**), 1554 (**2**) and 1428 (**1**), 1398 (**2**) cm^{-1} are assigned to the $\nu_{as}(COO)$ and $\nu_s(COO)$ modes of the carboxylate ligands, respectively.[42] The difference Δ ($\Delta = \nu_{as}(COO) - \nu_s(COO)$) for both complexes (142 cm^{-1} for **1**, 156 cm^{-1} for **2**) is less than that for NaO_2CMe (164 cm^{-1}) and NaO_2CPh (186 cm^{-1}), as expected for the bidentate bridging mode of the carboxylate ligation.[42] The existence of two types of benzoate ligands (monodentate,

(36) Castro, S. L.; Sun, Z.; Grant, C. M.; Bollinger, J. C.; Hendrickson, D. N.; Christou, G. *J. Am. Chem. Soc.* **1998**, *120*, 2365.

(37) (a) Ellis, T.; Glass, M.; Harton, A.; Folting, K.; Huffman, J. C.; Vincent, J. B. *Inorg. Chem.* **1994**, *33*, 5522. (b) Bino, A.; Chayat, R.; Pedersen, E.; Schneider, A. *Inorg. Chem.* **1991**, *30*, 856. (c) Donald, S.; Terrell, K.; Robinson, K. D.; Vincent, J. B. *Polyhedron* **1995**, *14*, 971.

(38) Pan, W.-Y.; Yu, X.-F. *Chin. J. Chem.* **1994**, *12*, 534.

(39) Representative references: (a) Bouwman, E.; Bolcar, M. A.; Libby, E.; Huffman, J. C.; Folting, K.; Christou, G. *Inorg. Chem.* **1992**, *31*, 5185. (b) Wemple, M. W.; Tsai, H.-L.; Wang, S.; Claude, J. P.; Streib, W. E.; Huffman, J. C.; Hendrickson, D. N.; Christou, G. *Inorg. Chem.* **1996**, *35*, 6437. (c) Aromi, G.; Bhaduri, S.; Artus, P.; Folting, K.; Christou, G. *Inorg. Chem.* **2002**, *41*, 805.

(40) Borer, L.; Thalken, L.; Ceccareli, C.; Glick, M.; Zhang, J. H.; Reiff, W. M. *Inorg. Chem.* **1983**, *22*, 1719.

(41) Grillone, M. D.; Benetollo, F.; Bombieri, G. *Polyhedron* **1991**, *10*, 2171.

(42) (a) Deacon, G. B.; Phillips, R. J. *Coord. Chem. Rev.* **1980**, *33*, 227. (b) Nakamoto, K. *Infrared and Raman Spectra of Inorganic and Coordination Compounds*, 4th ed.; Wiley: New York, 1986; pp 231−233, 251, 253.

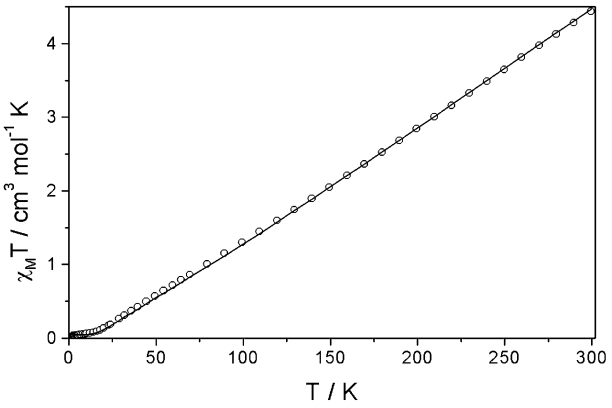

Figure 4. Plot of $\chi_M T$ vs T for a polycrystalline sample of complex **1**. The susceptibility, χ_M, was measured under a 0.1 T magnetic field. The solid line is a fit of the 2−300 K data to the appropriate 2J model; see the text for the fitting parameters.

Scheme 3

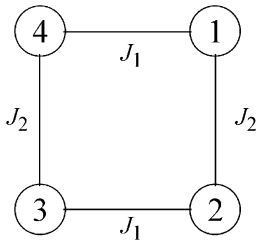

bidentate bridging) in **3** is reflected in its IR spectrum by the appearance of two ν_{as}(COO) bands at 1637 (monodentate) and 1558 cm^{-1} (bidentate bridging);[42] the two ν_s(COO) bands most probably coincide at 1402 cm^{-1}.

The spectra of **1** and **2** exhibit bands near 1100 and 625 cm^{-1}, due to the $\nu_3(F_2)$ and $\nu_4(F_2)$ modes of the uncoordinated T_d ClO_4^-, respectively;[42b] the $\nu_3(F_2)$ band in **2** should also involve a deformation phen or $PhCO_2^-$ character.

Magnetic Susceptibility Studies of 1−3. Variable-temperature magnetic susceptibility data were collected on analytically pure, powdered samples of complexes **1**−**3**. A plot of the product $\chi_M T$ of complex **1** vs temperature is shown in Figure 4 (χ_M is the corrected molar magnetic susceptibility/tetramer). The value of $\chi_M T$ decreases rapidly with decreasing temperature from 4.46 cm^3 mol^{-1} K at room temperature until a plateau of 0.035 cm^3 mol^{-1} K is reached at ∼16 K; the latter nonzero value is due to an amount of paramagnetic impurity. The temperature dependence of the susceptibility data reveals strong antiferromagnetic exchange interactions between the Fe^{III} atoms; in accord with this behavior, the room-temperature value of $\chi_M T$ is considerably less than expected for four noninteracting $S = 5/2$ metal centers (17.52 cm^3 mol^{-1} K). Inspection of the molecular structure of **1** reveals that there are two main exchange pathways. The first one, J_1, refers to the $Fe^{III}O(O_2CMe)_2Fe^{III}$ interactions, and the second one, J_2, refers to the $Fe^{III}(OH)Fe^{III}$ interactions. The exchange pathways in **1** are shown in Scheme 3. Thus, the Hamiltonian formalism given in eq 5 was used to fit the data, taking into account a small percentage of $S = 5/2$ paramagnetic impurity (ρ). The obtained fitting parameters

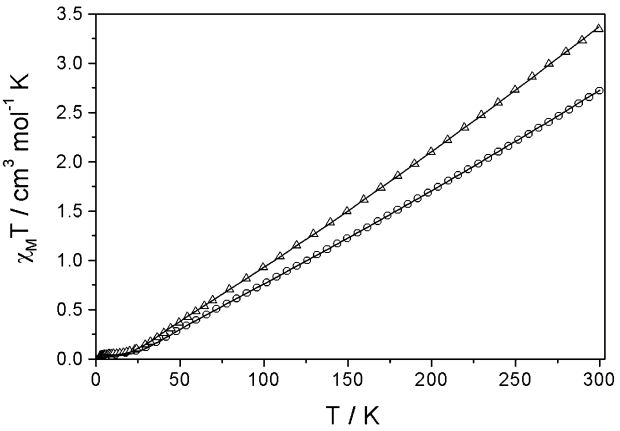

Figure 5. Plots of $\chi_M T$ vs T for microcrystalline samples of complexes **2** (open circles) and **3** (open triangles). The susceptibilities were measured under a 0.1 T magnetic field. The solid lines are the fits of the 2−300 K data to the appropriate 2J model; see the text for the fitting parameters.

are $J_1 = -75.4$ cm^{-1}, $J_2 = -21.4$ cm^{-1}, $g = 2.0(1)$, and $\rho = 0.8\%$.

$$H = -J_1(S_1S_4 + S_2S_3) - J_2(S_3S_4 + S_1S_2) \qquad (5)$$

A further verification for the amount of paramagnetic impurity comes from the plot of the reduced magnetization $M/N\mu_B$ vs the ratio of external magnetic field and the absolute temperature (HT^{-1}) at 2 K. The nonzero magnetization, although the ground state is $S = 0$, is in accordance with the small percentage of paramagnetic impurity found in the susceptibility data. The data were simulated using eq 6, where $B_{5/2}(x)$ is the theoretical Brillouin function for an $S = 5/2$ system and ρ the percentage impurity that has been found from the susceptibility measurements; the simulation is very good. The energies of the spin values obtained with the fitting values show that the first excited $S = 1$ state is well isolated from the diamagnetic $S = 0$ ground state ($\Delta E = 51$ cm^{-1}).

$$M = \rho N g \mu_B S B_{5/2}(x) \qquad (6)$$

The calculated J_1 and J_2 values are reasonable. Although there are few examples of complexes containing Fe^{III} atoms bridged solely by one μ-OH$^-$ group, there is, nonetheless, a particularly narrow range in which the J values are found (approximately −20 to −30 cm^{-1}).[30a,c] The value of J_2 in **1** (−21.4 cm^{-1}) is within the reported range. The value of J_1 (−75.4 cm^{-1}) is between the ranges previously reported for the (μ-oxo)bis(μ-acetato)- (−218 to −200 cm^{-1})[24a,25,43] and (μ-hydroxo)bis(μ-carboxylato)- (−16 to −60 cm^{-1})[2d,24a,b,c,d] diiron(III) cores. The intermediate J_1 value presumably reflects the nature of the bridge within the Fe(1)···Fe(4) and Fe(2)···Fe(3) pairs, which is neither pure (μ-OH)(μ-$O_2CMe)_2$ nor pure (μ-O)(μ-$O_2CMe)_2$, as reflected by the intermediate Fe−O(2, 4) distances (average 1.877(7) Å).[25b, 44]

Plots of the product $\chi_M T$ vs T for complexes **2** and **3** are shown in Figure 5. The data will not be discussed in detail

(43) (a) Arulsamy, N.; Glerup, J.; Hodgson, D. J. *Inorg. Chem.* **1994**, *33*, 3, 3043. (b) Jensen, K. B.; McKenzie, C. J.; Simonsen, O.; Toftlund, H.; Hazell, A. *Inorg. Chim. Acta* **1997**, *257*, 163.
(44) Werner, R.; Ostrovsky, S.; Griesar, K.; Haase, W. *Inorg. Chim. Acta* **2001**, *326*, 78.

Scheme 4

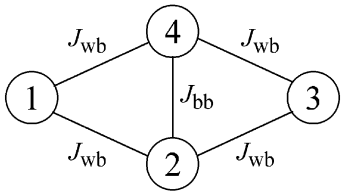

since magnetic studies with similar structures have been previously reported.[9a,d,e,15a,b] The room-temperature values are 2.72 $cm^3\ mol^{-1}$ K for **2** and 3.36 $cm^3\ mol^{-1}$ K for **3**, both being lower than the value expected for four uncoupled 5/2 spins. The values of $\chi_M T$ decrease monotonically with decreasing temperature until a plateau of 0.04 $cm^3\ mol^{-1}$ K (essentially diamagnetic value) is reached for both complexes at 16 K; the residual $\chi_M T$ value is due to a similar percentage of paramagnetic impurity in both complexes. The data suggest antiferromagnetically coupled systems with $S = 0$ ground state. For a complex such as **2** a total of five exchange parameters J_{ij} are required to cover each possible pairwise exchange interaction between Fe^{III} atoms *i* and *j*; a sixth parameter J_{13} (the numbering scheme is the same as that shown in Figure 2) is assumed to be zero, given the large distance involved (Fe(1)···Fe(3) = 5.880(2) Å). However, the main exchange interaction pathway will be via the μ_3-O^{2-} bridges, not the benzoate bridges, so that from the magnetism viewpoint, the core symmetry is reduced and only three *J* values are required, $J_{12} = J_{14} = J_{wb}$, $J_{23} = J_{34} = J'_{wb}$, and $J_{24} = J_{bb}$, where b = body and w = wing-tip. In fact, consideration of the Fe−O and Fe−O−Fe distances and angles in Table 3 shows that the almost same pyramidality of O(1) and O(2) has a minor influence on these structural parameters and a 2*J* model appropriate for C_{2v} symmetry, i.e., $J_{wb} = J'_{wb}$, thus does not appear unreasonable. Analogous considerations can be applied to **3**, for which, due to symmetry, a total of three exchange parameters are initially required to cover each possible pairwise interaction between the Fe^{III} atoms (assuming that $J_{11'} = 0$; see Figure 3). This model is also the one employed previously for complex $[Fe_4O_2(O_2CMe)_7(bpy)_2](ClO_4)$ and discussed in detail elsewhere.[9a] The exchange pathways in **2** are shown in Scheme 4; bearing in mind that Fe(4) = Fe(2′), Fe(1) = Fe(1′), and Fe(3) = Fe(1), a similar interaction scheme applies to **3**. The Hamiltonian formalism given in eq 7 was used to fit the data taking into account a small percentage of $S = 5/2$ paramagnetic impurity (ρ). The obtained fitting parameters are $J_{bb} = -2.4\ cm^{-1}$, $J_{wb} = -77.6\ cm^{-1}$, $g = 2.0$, and $\rho = 1\%$ for **2** and $J_{bb} = -15.6\ cm^{-1}$, $J_{wb} = -65.7\ cm^{-1}$, $g = 2.0$, and $\rho = 1\%$ for **3**. The energy difference between the $S = 0$ ground state and the first excited $S = 1$ state is 78 cm^{-1} for **2** and 66 cm^{-1} for **3**. The different *J* parameters derived for **2** and **3** arise from the structural differences between the two complexes, the main difference being the absence of the benzoate group in **3** that bridges the body Fe^{III} sites. The obtained *J* values can be compared with those previously determined, for example, in $[Fe_4O_2(O_2CMe)_7(bpy)_2](ClO_4)$ ($J_{bb} = -17.8\ cm^{-1}$, $J_{wb} = -91.0\ cm^{-1}$, $g = 2.0$)[9a] and $[Fe_4O_2(O_2CEt)_7(bpy)_2](PF_6)$ ($J_{bb} = -14.6\ cm^{-1}$, $J_{wb} = -83.2\ cm^{-1}$, $g = 2.02$).[9d] As for $[Fe_4O_2(O_2CMe)_7(bpy)_2](ClO_4)$, an error-surface plot for the fitting in **2** and **3** shows that while the value of J_{wb} is well determined by the fitting procedure, the value of J_{bb} is not; since J_{wb} is so much stronger than J_{bb} and since there are four J_{wb} interactions and only one J_{bb}, the spin-manifold energies are primarily determined by J_{wb}, making the precise value of J_{bb} indeterminate. Thus, as for the bpy complex, a large range of J_{bb} values give essentially equally good fits of the data, although the quoted J_{bb} values give the lowest fitting error. Tetranuclear butterfly iron(III) complexes, such as **2**, **3**, $[Fe_4O_2(O_2CMe)_7(bpy)_2](ClO_4)$,[9a] and related species,[15a,b] are regarded as examples exhibiting spin frustration.[9a,45] The strong antiferromagnetic J_{wb} interactions frustrate the weaker J_{bb} interaction leading to the $S = 0$ ground state via the spin alignments shown pictorially in Scheme 5; i.e., the Fe_b spins are parallel in the ground state even though the J_{bb} parameter is most likely negative (antiferromagnetic).[9d,10]

Scheme 5

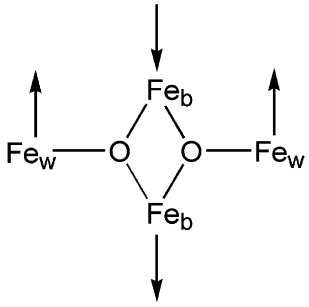

$$H = -2J_{bb}(S_2S_4) - J_{wb}[(S_2 + S_4)(S_1 + S_3)] \qquad (7)$$

The $S = 0$ ground state of complexes **1**−**3** is not surprising; this a very common ground state for Fe_x^{III} clusters, where *x* is an even number.[10,24e,23a,45] Some important exceptions, however, include cations $[Fe_8O_2(OH)_{12}(tacn)_6]^{8+}$ ($S = 10$, tacn = triazacyclonane),[2e,3,46] compound $[Fe_4(OMe)_6(dpm)_6]$ ($S = 5$),[4] and complex $[Fe_6O_2(OH)_2(O_2CMe)_{10}L_2]$ ($S = 5$, L^- is the anion of 1,1-bis(*N*-methylimidazol-2-yl)-1-hydroxypropane[2d]).

EPR Spectra. X-band powder EPR spectra of **1**−**3** were recorded in a wide range of temperatures (300−4 K). The spectra are nearly identical. The spectrum of **1** at 4 K is

(45) (a) Gatteschi, D.; Caneschi, A.; Sessoli, R.; Cornia, A. *Chem. Soc. Rev.* **1996**, *25*, 101. (b) Winpenny R. E. P. *Acc. Chem. Res.* **1997**, *30*, 89. (c) Benelli, C.; Parsons, S.; Solan, G. A.; Winpenny, R. E. P. *Angew. Chem., Int. Ed. Engl.* **1996**, *35*, 1825. (d) Brechin, E. K.; Knapp, M. J.; Huffman, J. C.; Hendrickson, D. N.; Christou, G. *Inorg. Chim. Acta* **2000**, *297*, 389. (e) Seddon, E. J.; Yoo, J.; Folting, K.; Huffman, J. C.; Hendrickson, D. N.; Christou, G. *J. Chem. Soc., Dalton Trans.* **2000**, 3640. (f) Ammala, P.; Cashion, J. D.; Kepert, C. M.; Moubaraki, B.; Murray, K. S.; Spiccia, L.; West, B. O. *Angew. Chem., Int. Ed.* **2000**, *39*, 1688.

(46) (a) Barra, A.-L.; Debrunner, P.; Gatteschi, D.; Schulz, C. E.; Sessoli, R. *Europhys. Lett.* **1996**, *35*, 133. (b) Sangregorio, C.; Ohm, T.; Paulsen, C.; Sessoli, R.; Gatteschi, D. *Phys. Rev. Lett.* **1997**, *78*, 1997. (c) Caneschi, A.; Ohm, T.; Paulsen, C.; Rovai, D.; Sangregorio, C.; Sessoli, R. *J. Magn. Magn. Mater.* **1998**, *177*−*181*, 1330. (d) Caciuffo, R.; Amoretti, G.; Murani, A.; Sessoli, R.; Caneschi, A.; Gatteschi, D. *Phys. Rev. Lett.* **1998**, *81*, 4744. (e) Gatteschi, D.; Lascialfari, A.; Borsa, F. *J. Magn. Magn. Mater.* **1998**, *185*, 238. (f) Wernsdorfer, W.; Caneschi, A.; Sessoli, R.; Gatteschi, D.; Cornia, A.; Villar, V.; Paulsen, C. *Phys. Rev. Lett.* **2000**, *84*, 2965.

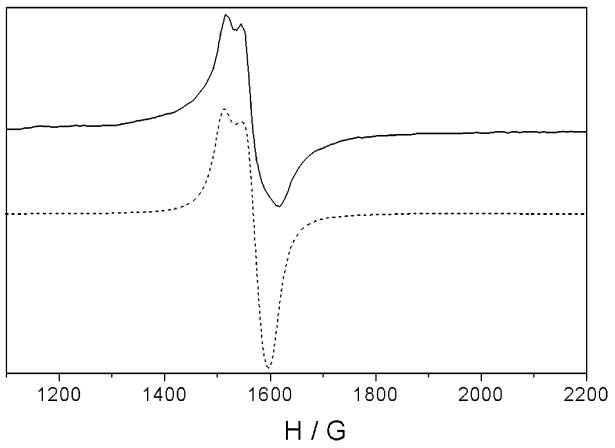

Figure 6. X-band EPR spectrum of a polycrystalline sample of **1** at 4 K (solid line) along with the simulated one (dotted line) according to eq 8. See the text for details.

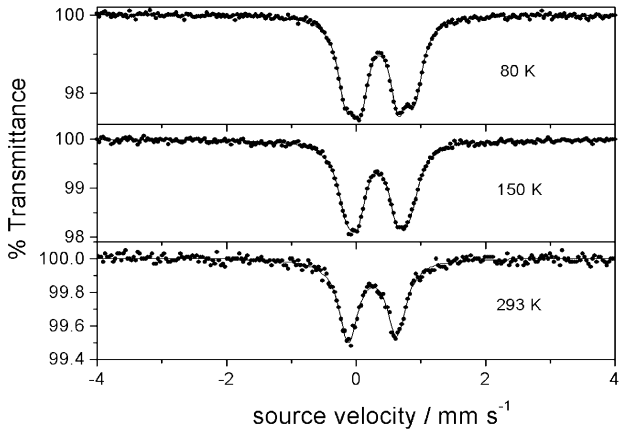

Figure 7. Variable-temperature ^{57}Mössbauer spectrum for complex **1**.

shown in Figure 6. The spectra show a signal at $g = \sim 4.3$. This resonance, which has a rhombic character, is the signature of an $S = 5/2$ state, indicating the presence of a paramagnetic impurity in the samples. A simulation was carried out using the Hamiltonian given in eq 8; the simulated spectrum is also presented in Figure 6. The simulated parameters are $D = 0.26$ cm^{-1}, $E = 0.0858$ cm^{-1} ($\lambda = 0.33$), and $g = 2.02$.

$$\hat{H} = g\mu_B S \cdot H + S \cdot D \cdot S \qquad (8)$$

^{57}Fe Mössbauer Spectroscopy. Mössbauer spectra for complexes **1**−**3** were recorded at 80, 150, and 293 K. The spectra of **1** and **3** are shown in Figures 7 and 8, respectively. The spectra were least-squares fitted with Lorentzian lines, and the resulting isomer shift (δ) and quadrupole splitting (ΔE_Q) parameters (Table 6) are consistent with the presence of high-spin Fe(III) centers in non-sulfur environments.[47]

Despite the close similarity of the four Fe^{III} centers in the rectangular core of **1**, the low-temperature spectra consist of two quadrupole-split doublets of approximately equal absorption areas; see Figure 7. The isomer shift values at 80 K ($\delta_A = 0.470(1)$, $\delta_B = 0.485(2)$ mm s^{-1}) are very close

(47) (a) Murray, K. S. *Coord. Chem. Rev.* **1974**, *12*, 1. (b) Greenwood, N. N.; Gibb, T. C. *Mössbauer Spectroscopy*; Chapman and Hall: London, 1971; pp 148−164.

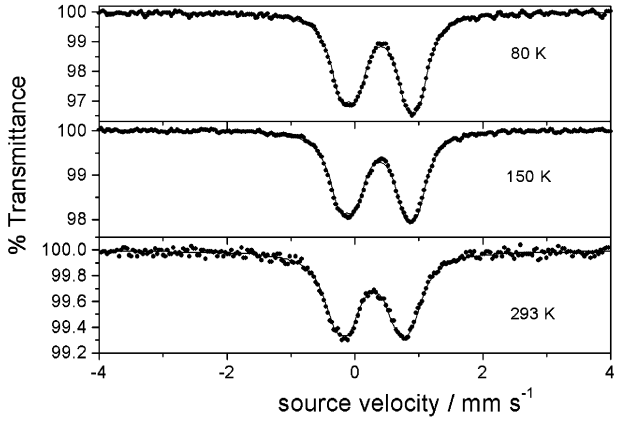

Figure 8. Variable-temperature ^{57}Mössbauer spectrum for complex **3**.

Table 6. Mössbauer Paremeters for Complexes **1**−**3**

compd site	T (K)	area ratio (%)	δ^a (mm s^{-1})	$\Gamma_{1/2}{}^b$ (mm s^{-1})	ΔE_Q (mm s^{-1})
1A[c]	80	53.6(6)	0.470(1)	0.144(2)	0.573(4)
1A[c]	150	57(1)	0.443(2)	0.154(2)	0.614(7)
1B	80	46.4(6)	0.485(2)	0.144(2)	1.032(4)
1B	150	43(1)	0.456(2)	0.154(2)	0.971(8)
1(A + B)[c,d]	293	100	0.370(3)	0.172(4)	0.717(5)
2b	80	46.2(6)	0.540(1)	0.161(2)	0.822(4)
2b	150	46(1)	0.507(2)	0.161(3)	0.803(7)
2b	293	50(3)	0.440(6)	0.161[e]	0.74(2)
2w	80	53.8(6)	0.494(1)	0.161(2)	1.262(4)
2w	150	54(1)	0.465(2)	0.161(3)	1.252(6)
2w	293	49(3)	0.403(6)	0.161[e]	1.19(2)
3b	80	49(3)	0.527(2)	0.182(5)	0.74(1)
3b	150	48(3)	0.500(2)	0.184(5)	0.74(1)
3b	293	49(1)	0.404(4)	0.222(9)	0.72(1)
3w	80	51(3)	0.502(2)	0.183(5)	1.189(1)
3w	150	52(3)	0.479(2)	0.187(5)	1.18(1)
3w	293	51(1)	0.400(4)	0.227(9)	1.14(1)

[a] Isomer shift relative to iron foil at room temperature. [b] Width at half-height. [c] Arbitrary notation: site A is the most symmetrical. [d] Data could not be fitted by two doublets due to close proximity of peaks. [e] Parameter values fixed. b = body, and w = wing-tip.

to each other, as expected for very similar N_2O_4 ligand environments for the Fe^{III} centers. However, the quadrupole splitting values at 80 K ($\Delta E_{QA} = 0.573(4)$, $\Delta E_{QB} = 1.032(4)$ mm s^{-1}) clearly indicate a quite different symmetry for these N_2O_4 environments. Due to second-order Doppler effect,[47b] both δ_A and δ_B values slightly decrease with increasing temperature, whereas ΔE_{QA} and ΔE_{QB} converge to a common average value yielding a unique quadrupole-split doublet at room temperature. The large difference in ΔE_Q values for sites A and B at 80 K points out to quite different local symmetries for the two ferric sites: splitting of the T_{2g} orbital triplet by crystal field distortions affording lower than octahedral symmetry is significantly larger for site B compared to site A.

Thus, we may consider that the tetranuclear metal core of **1** assumes a less symmetric conformation at 80 K than at 293 K and that the 80 K conformation imposes a less symmetric environment to two metal centers (site B) compared to the other ones (site A). Given the flexibility of the OHO^{3-} moiety, where the proton is hydrogen bonded to two "oxide" ions (O(2) and O(4) in Figure 1), a conformational isomerism due to thermal motion of this proton as depicted in Scheme 6 may be considered. Partial localization

Scheme 6

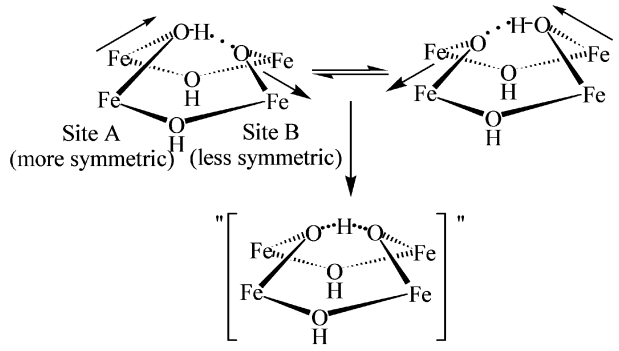

of the proton toward one of these "oxide" ions would endow this ion with a strong hydroxo character, thus elongating the corresponding Fe−O bonds; the resulting stronger oxo character for the other "oxide" ion of the OHO^{3-} bridge would induce a shortening of the other two Fe−O bonds. Assuming that the Fe−(μ-$O_{hydroxo}$), i.e., Fe−O(1) and Fe−O(3), Fe−N, and Fe−$O_{acetate}$ bonds are almost identical for the two conformations, the above-mentioned process would result in Fe−(μ-$O_{"oxide"}$) distances closer to Fe−(μ-OH) than to Fe−(μ-O) distances for one Fe_2(μ-$O_{"oxide"}$)(μ-$O_2CMe)_2$ unit (thus yielding a more symmetric environment for the corresponding Fe^{III} centers (site A)); conversely, the Fe−(μ-$O_{"oxide"}$) distances in the other Fe_2(μ-$O_{"oxide"}$)(μ-O_2-$CMe)_2$ dinuclear unit would be closer to Fe−(μ-O) than to Fe−(μ-OH) distances (thus yielding a less symmetric environment for the corresponding Fe^{III} centers (site B)). At low temperature, the reduced thermal motion may slow the process to such an extent that the resulting small difference in coordination environments can be detected through such a sensitive technique as Mössbauer spectroscopy. In the high-temperature range (T > 200 K), the process is thermally accelerated to such an extent that an averaged coordination environment can only be observed. In the room-temperature structure of **1**, the average distance for the Fe−(μ-$O_{"oxide"}$) bonds (Fe(2, 3)−O(2), Fe(1, 4)−O(4)) is 1.877(7) Å, while the ranges reported for the Fe^{III}−$O_{oxo/hydroxo}$ bonds in the $[Fe_2(\mu\text{-O})(\mu\text{-}O_2CR)_2]^{2+}$ and $[Fe_2(\mu\text{-OH})(\mu\text{-}O_2CR)_2]^{3+}$ units are 1.76−1.82[8a,24a,25] and 1.93−1.98 Å,[2c,d,14,24b,c] respectively.

The Mössbauer spectra of complexes **2** and **3** consist of two quadrupole-split doublets of equal areas. The two doublets are assigned to the body and wing-tip pairs of iron(III) atoms. The isomer shift values allow one to distinguish the O_6 donor set of the body Fe^{III} centers from the N_2O_4 donor set of the wing-tip Fe^{III} centers (at 80 K: δ_{body} = 0.540(1), $\delta_{wing-tip}$ = 0.494(1) mm s^{-1} for **2**; δ_{body} = 0.527(2), $\delta_{wing-tip}$ = 0.502(2) mm s^{-1} for **3**). These δ values show little temperature dependence due to second-order Doppler effect.[47b] This assignment is confirmed in terms of coordination environment symmetry, in agreement with previous observations for similar butterfly cores.[9e] The ΔE_Q values for both sites in **2** and **3** reflect deviations from octahedral geometry, since the valence-electron contribution to ΔE_Q is negligible for a high-spin Fe^{III} ion. The two ΔE_Q values for each spectrum are also significantly different. For complex **2**, the doublet with larger ΔE_Q (~ 1.2 mm s^{-1}) is assigned to the wing-tip Fe(1) and Fe(3) (see Figure 2) that

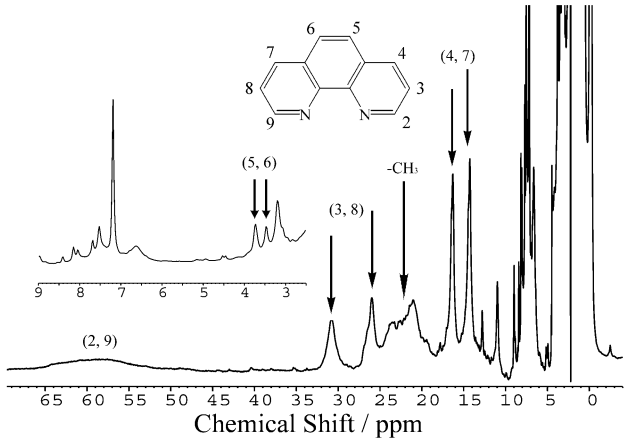

Figure 9. ^{1}H NMR (400 MHz) spectrum of complex **1** in $CDCl_3/CD_3CN$ (6:1 v/v). An expansion of the 2.5−9.0 ppm region is shown separately.

have $Fe^{III}N_2O_4$ coordination spheres and the larger range of bond length (1.807(6)−2.169(8) Å). The short Fe(1)−O(1) (1.819(6) Å) and Fe(3)−O(2) (1.807(6) Å) bonds for the wing-tip Fe^{III} ions of **2** provide the main distortion of the coordination geometry from octahedral and are thus the main contributors to the greater ΔE_Q value.[9e] In contrast, the body Fe(2) and Fe(4) (see Figure 2) have an FeO_6 environment and a narrower range of bond length (1.916(4)−2.062(6) Å); the doublet assigned to these body metal ions has ΔE_Q = ~0.8 mm s^{-1}. Analogous arguments are valid for complex **3**, where again the doublet with larger ΔE_Q (~1.2 mm s^{-1}) is assigned to the wing-tip Fe(1) and Fe(1′) (see Figure 3). Somewhat similar ΔE_Q differences were observed between wing-tip and body Fe^{III} ions in $[Fe_4O_2(O_2CMe)_7(bpy)_2](ClO_4)$[9a] (1.333(3)/0.962(4) mm s^{-1} at 105 K) and other butterfly-type complexes with the $[Fe_4(\mu_3\text{-}O)_2]^{8+}$ core (**I**),[15b] exhibiting large differences in Fe^{III}−O^{2-} bond lengths between wing-tip and body metal ions.

^{1}H NMR Spectroscopy. An ^{1}H NMR study of complexes **1**−**3** has been carried out. This study has been conducted to investigate whether the solid-state structure of the complexes is retained in solution. In addition, NMR has represented a useful tool to monitor the various transformations discussed in the synthetic section and the purity of the products. In Figures 9 and 10 are shown spectra recorded for **1** and **2**; the measured chemical shifts are collected in Table 7. Assignments have been assisted by literature reports.[9a,10,11,13,15a,24c,48] The spectra display broadened and shifted resonances, features typical of paramagnetic NMR.

The ^{1}H NMR spectrum of **1** in CD_3CN covers the 0−70 ppm region being extremely complicated, thus indicating the existence of several species in solution. Spectra recorded in a $CDCl_3/CD_3CN$ (6:1 v/v) solvent mixture (**1** is insoluble in pure $CDCl_3$) were simpler and better defined. Eight peaks are assignable to the coordinated phen protons. It is not clear if these peaks correspond to the eight protons of a given phen (in such a case all coordinated phen ligands are magnetically equivalent) or to the four proton types of two nonequivalent phen ligands (in such a case the protons

(48) Chen, Q.; Lynch, J. B.; Gomez-Romero, P.; Ben-Hussein, A.; Jameson, G. B.; O'Connor, C. J.; Que, L., Jr. *Inorg. Chem.* **1988**, *27*, 2673.

Table 7. ^{1}H NMR Spectral Data[a] for Complexes **1**−**3**

complex	phen[e]	RCO_2^-
1[b] (R = Me)	57.8, 62.4 (2, 9), 30.8, 25.6 (3, 8), 16.2, 14.2 (4, 7), 3.7, 3.5 (5, 6)	20−24
2[c] (R = Ph)	*40.1*, *34.4*/38.15, 32.85 (2, 9), *21.2*, *17.4*/20.4, 16.9 (3, 8), *13.2*, *11.4*/12.9, 11.2 (4, 7), *6.3*, *5.8*/6.3, 5.8 (5, 6)	*9.1*/9.0, *7.9*/8.0, *7.8*/7.8, *7.5*/7.4, *7.4*/7.2
3[d] (R = Ph)	82.1, 69.2 (2, 9), 36.0, 31.9 (3, 8), 21.2, 14.5 (4, 7), 14.0, 11.9 (5, 6)	6−10.5

[a] The data are the chemical shifts (ppm) on the δ scale. [b] In $CDCl_3/CD_3CN$ (6:1 v/v). [c] In $CDCl_3$; shifts observed in pure CD_3CN are shown in italics. [d] In CD_3CN. [e] Numbers in parentheses refer to the phen ring positions.

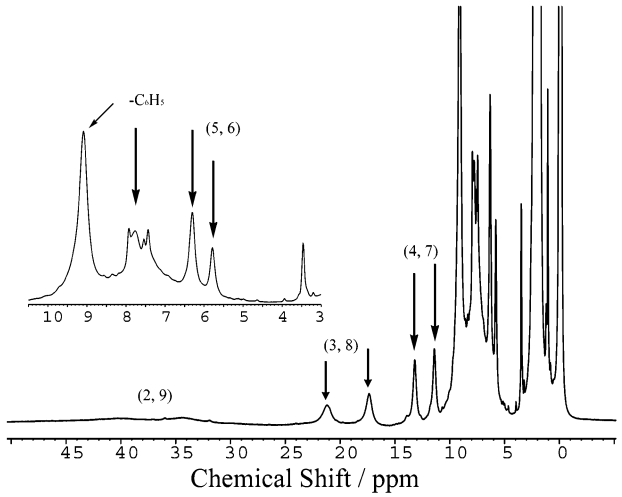

Figure 10. ^{1}H NMR (400 MHz) spectrum of complex **2** in $CDCl_3$. An expansion of the 3.0−10.5 ppm region is shown separately.

belonging to each 2, 9/3, 8/4, 7/5, 6 pair of each independent phen are equivalent and would appear as a single peak). Consideration of peak widths allows for assignment of the very broad resonance at 57.8 ppm and the shoulder at 62.4 ppm as being due to the 2, 9 protons, since they are closest to the metal centers. Along the same lines, the most peripheral phen protons should give rise to very narrow and less hyperfine shifted peaks; the peaks at 3.7 and 3.5 ppm are thus assigned to the 5, 6 protons. The two broad peaks at 30.8 and 25.6 ppm are assigned to the 3, 8 protons, while the relatively narrow peaks at 16.2 and 14.2 ppm must be due to the 4, 7 protons. Finally, a group of signals observed in the 20−24 ppm region could be attributed[10] to the acetate protons.

For complex **2**, spectra recorded in CD_3CN and $CDCl_3$ were relatively simple and well defined. The solvent dependence of the spectra is small (Table 7). The peaks of the phen protons exhibit a pattern similar to that of **1**, and their assignments were carried out in a similar fashion. Five peaks in the 9.1−7.2 ppm region are attributed[15a,48] to the phenyl ring protons of the benzoate bridges; specific assignments of these resonances are difficult. In the spectrum of complex **3** in CD_3CN the observed chemical shifts span a larger range (up to ∼70 ppm wide); however, the pattern of the peaks is similar to that observed in **2**.

In summary, the above ^{1}H NMR study has shown that the solid-state structures of $[Fe_4(OHO)(OH)_2(O_2CMe)_4(phen)_4]^{3+}$, $[Fe_4O_2(O_2CPh)_7(phen)_2]^+$, and $[Fe_4O_2(O_2CPh)_8(phen)_2]$ are most probably retained in $CDCl_3/CD_3CN$ (6:1 v/v), $CDCl_3$ and CD_3CN, and CD_3CN, respectively.

Summary and Perspectives

The use of 1,10-phenanthroline (phen) in Fe^{III} carboxylate chemistry has provided access to three new tetranuclear iron(III) complexes. Complex **1** contains the unprecedented $[Fe_4(\mu_4\text{-OHO})(\mu\text{-OH})]^{7+}$ core. This complex fulfils the prediction in the Introduction where we stated that there appeared no reason 1:1 Fe^{III} carboxylate/phen assemblies should not be made. The identification of **1** emphasizes the belief that the Fe^{III}/O^{2-}, $OR'^-/RCO_2^-/L-L$ chemistry (R′ = H, Me, ...; L−L = bpy, phen) is rich and exciting. Complexes **2** and **3** have the well-known $[Fe_4(\mu_3\text{-O})_2]^{8+}$ core not previously described with phen. Our efforts have also demonstrated that the replacement of the body−body carboxylate bridge (present in **2**) by two terminal monodentate carboxylates (present in **3**) is easy. These could have future utility as sites for incorporation of other ligands by metathesis or as means to obtain higher nuclearity compounds. Although the three reported complexes have been found to possess $S = 0$ ground states, they nevertheless suggest possibilities for other Fe_x species that might exist and which may have high-spin ground states. We are trying to prepare such species by (i) introducing alkoxo ligands that can lead to new Fe_x topologies not accessible with O^{2-} and RCO_2^- ligands alone, (ii) replacing μ-OH^-/μ-OR'^- ligands (which often cause antiferromagnetic interactions) in known clusters by end-on azido ligands (which propagate ferromagnetic exchange interactions), or/and (iii) incorporating aromatic heterocycles that can simultaneously chelate and bridge Fe^{III} ions.

Acknowledgment. This work was supported by the Greek General Secretariat of Research and Technology (Grant 99ED139). A.K.B. thanks the European Community for partial support through a postdoctoral grant within the framework of the TMR contract FMRX-CT980174. We thank Prof. D. Gatteschi (Department of Chemistry, University of Florence, Florence, Italy) for permitting us to collect variable-temperature magnetic susceptibility data at his laboratory and for helpful discussions.

Supporting Information Available: X-ray crystallographic data in CIF format for the structures of complexes **2**·2MeCN and **3**·$2H_2O$ and information concerning the program used to derive the susceptibility equation for complex **1**·4.4MeCN·H_2O (including a table with the experimental and calculated susceptibilities). This material is available free of charge via the Internet at http://pubs.acs.org.

IC025795K